

Measurement of the W-boson mass with the ATLAS detector

N. Andari

University of Birmingham

May 3, 2017

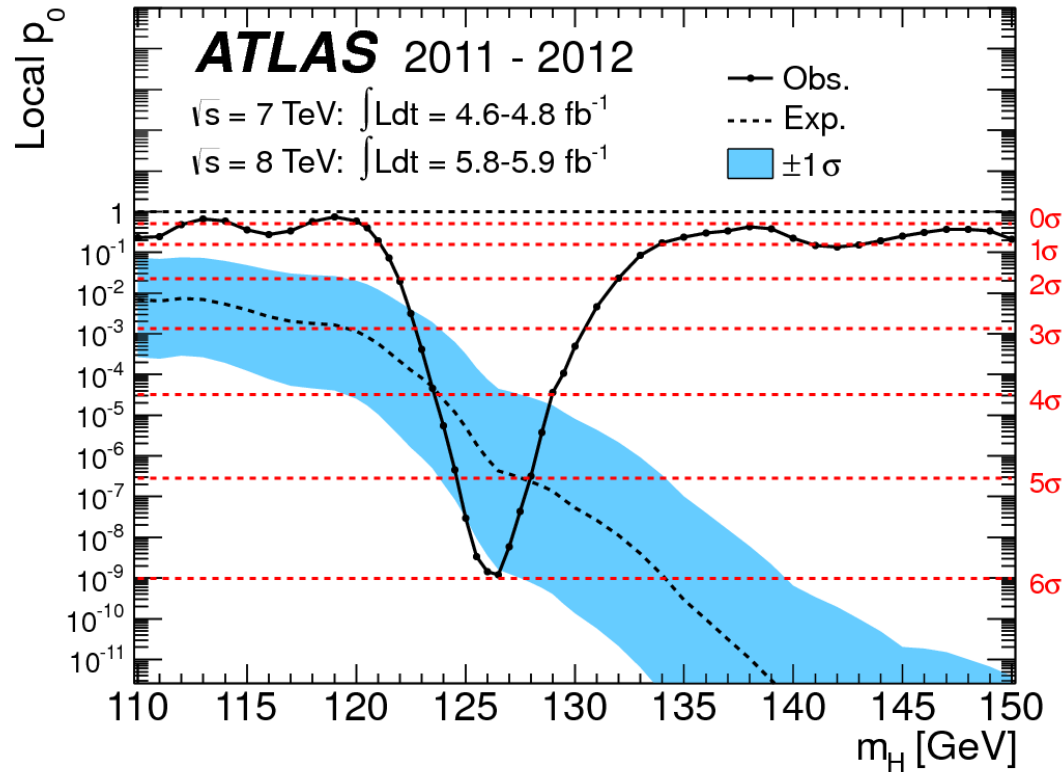


Standard Model

Seminar 4 July 2012

Huge step in our understanding of Particle Physics:
recent discovery of the Higgs boson

[Phys. Lett. B 716 \(2012\) 1-29](#)



SM puzzle completed, but many open questions (mass hierarchy, baryon asymmetry, dark matter...) remain without answers → **Search for Beyond the SM**



Beyond the Standard Model

Direct searches: huge numbers of new results - astonishing achievement.
No significant signals - updated limits. More still to come with 13 TeV.

ATLAS SUSY Searches* - 95% CL Lower Limits

Status: March 2017

Model	$\epsilon, \mu, \tau, \gamma$	Jets	E_{miss}^T	$\int \mathcal{L} dt [fb^{-1}]$	Mass limit	$\sqrt{s} = 7, 8 \text{ TeV}$	$\sqrt{s} = 13 \text{ TeV}$	Reference
Inclusive Searches								
MSUGRA/CMSM	$0 < \epsilon, \mu < 1-2$	2-10 jets/3 b	Yes	20.3	1.85 TeV	1.57 TeV	1.05 TeV	1507.0525
$\tilde{g}\tilde{g} \rightarrow g\tilde{g}$	mono-jet	0-2 jets	Yes	36.1	608 GeV	1.57 TeV	1.05 TeV	ATLAS-CONF-2017-022
$\tilde{g}\tilde{g} \rightarrow g\tilde{g}$ (compressed)	mono-jet	1-3 jets	Yes	3.2	2.02 TeV	2.01 TeV	1.7 TeV	1604.0773
$\tilde{g}\tilde{g} \rightarrow g\tilde{g}$	0-2 jets	Yes	36.1	2.01 TeV	2.01 TeV	1.7 TeV	1.05 TeV	ATLAS-CONF-2017-022
$\tilde{g}\tilde{g} \rightarrow g\tilde{g}$	3 μ jets	Yes	13.2	1.7 TeV	1.7 TeV	1.05 TeV	1.05 TeV	ATLAS-CONF-2016-037
$\tilde{g}\tilde{g} \rightarrow g\tilde{g}$	0-3 jets	Yes	13.2	1.8 TeV	1.8 TeV	1.05 TeV	1.05 TeV	ATLAS-CONF-2016-037
GMSB (\tilde{t} NLSP)	$1.2 + 0.1 \ell$	0-2 jets	Yes	3.2	2.0 TeV	2.0 TeV	1.05 TeV	1607.0579
GGM (bino NLSP)	2 γ	Yes	3.2	1.85 TeV	1.85 TeV	1.05 TeV	1.05 TeV	1606.09150
GGM (higgsino-bino NLSP)	1 b	Yes	20.3	1.37 TeV	1.37 TeV	1.05 TeV	1.05 TeV	1507.05493
GGM (higgsino-bino NLSP)	2 jets	Yes	13.3	1.8 TeV	1.8 TeV	1.05 TeV	1.05 TeV	ATLAS-CONF-2016-066
GGM (higgsino NLSP)	2 μ jets	Yes	20.3	900 GeV	900 GeV	1.05 TeV	1.05 TeV	1503.0320
Gravitino LSP	mono-jet	Yes	20.3	865 GeV	865 GeV	1.05 TeV	1.05 TeV	1502.01518
3γ gen sources direct production								
$\tilde{g}\tilde{g} \rightarrow g\tilde{g}$	0-1 μ jets	3 b	Yes	36.1	1.92 TeV	1.92 TeV	1.05 TeV	ATLAS-CONF-2017-021
$\tilde{g}\tilde{g} \rightarrow g\tilde{g}$	0-1 μ jets	3 b	Yes	20.1	1.37 TeV	1.37 TeV	1.05 TeV	ATLAS-CONF-2017-021
$\tilde{g}\tilde{g} \rightarrow g\tilde{g}$	0-1 μ jets	3 b	Yes	20.1	1.37 TeV	1.37 TeV	1.05 TeV	1407.0600
$\tilde{g}\tilde{g} \rightarrow g\tilde{g}$	0-2 jets	Yes	3.2	840 GeV	840 GeV	1.05 TeV	1.05 TeV	1606.08772
$\tilde{g}\tilde{g} \rightarrow g\tilde{g}$	2 μ jets	1 b	Yes	13.2	325-685 GeV	325-685 GeV	1.05 TeV	ATLAS-CONF-2016-037
$\tilde{g}\tilde{g} \rightarrow g\tilde{g}$	0-2 μ jets	1-2 b	Yes	4.7/13.3	117-170 GeV	200-730 GeV	1.05 TeV	1209.2102, ATLAS-CONF-2016-077
$\tilde{g}\tilde{g} \rightarrow g\tilde{g}$	0-2 μ jets	0-2 jets/1-2 b	Yes	20.3	90-195 GeV	205-950 GeV	1.05 TeV	1506.0816, ATLAS-CONF-2017-039
$\tilde{g}\tilde{g} \rightarrow g\tilde{g}$	0-2 jets	Yes	3.2	90-323 GeV	150-600 GeV	1.05 TeV	1.05 TeV	1604.0773
$\tilde{g}\tilde{g} \rightarrow g\tilde{g}$	2 μ jets	1 b	Yes	20.3	290-760 GeV	290-760 GeV	1.05 TeV	1403.3222
$\tilde{g}\tilde{g} \rightarrow g\tilde{g}$	3 μ jets	1 b	Yes	36.1	200-760 GeV	200-760 GeV	1.05 TeV	ATLAS-CONF-2017-019
$\tilde{g}\tilde{g} \rightarrow g\tilde{g}$	1-2 μ jets	4 b	Yes	36.1	300-590 GeV	300-590 GeV	1.05 TeV	ATLAS-CONF-2017-019
EW direct								
$\tilde{g}\tilde{g} \rightarrow g\tilde{g}$	2 μ jets	0	Yes	20.3	90-335 GeV	90-335 GeV	1.05 TeV	1403.5294
$\tilde{g}\tilde{g} \rightarrow g\tilde{g}$	2 μ jets	0	Yes	13.3	640 GeV	640 GeV	1.05 TeV	ATLAS-CONF-2016-096
$\tilde{g}\tilde{g} \rightarrow g\tilde{g}$	2 μ jets	0	Yes	14.8	580 GeV	580 GeV	1.05 TeV	ATLAS-CONF-2016-096
$\tilde{g}\tilde{g} \rightarrow g\tilde{g}$	3 μ jets	0	Yes	13.2	1.0 TeV	1.0 TeV	1.05 TeV	ATLAS-CONF-2016-096
$\tilde{g}\tilde{g} \rightarrow g\tilde{g}$	2-3 μ jets	0-2 jets	Yes	20.3	425 GeV	425 GeV	1.05 TeV	1403.5294, 1402.7029
$\tilde{g}\tilde{g} \rightarrow g\tilde{g}$	2-3 μ jets	0-2 jets	Yes	20.3	270 GeV	270 GeV	1.05 TeV	1501.07110
$\tilde{g}\tilde{g} \rightarrow g\tilde{g}$	4 μ jets	0	Yes	20.3	635 GeV	635 GeV	1.05 TeV	1405.3086
GGM (bino NLSP) weak prod.	1 μ jet	Yes	20.3	115-370 GeV	115-370 GeV	1.05 TeV	1.05 TeV	1507.05493
GGM (bino NLSP) weak prod.	2 γ	Yes	20.3	590 GeV	590 GeV	1.05 TeV	1.05 TeV	1507.05493
Long-lived particles								
Direct $\tilde{g}\tilde{g} \rightarrow g\tilde{g}$ prod., long-lived \tilde{g}	Disapp. trk	1 jet	Yes	36.1	430 GeV	430 GeV	1.05 TeV	ATLAS-CONF-2017-017
Direct $\tilde{g}\tilde{g} \rightarrow g\tilde{g}$ prod., long-lived \tilde{g}	dE/dx trk	Yes	18.4	495 GeV	495 GeV	1.05 TeV	1.05 TeV	1506.09332
Stable stopped \tilde{g} R-hadron	0	1-5 jets	Yes	27.9	850 GeV	850 GeV	1.05 TeV	1310.0884
Metastable \tilde{g} R-hadron	trk	-	-	3.2	1.87 TeV	1.87 TeV	1.05 TeV	1600.05120
GMSB, stable \tilde{g} , long-lived \tilde{g}	dE/dx trk	-	-	3.2	1.57 TeV	1.57 TeV	1.05 TeV	1604.04420
GMSB, $\tilde{g} \rightarrow g\tilde{g}$, long-lived \tilde{g}	1-2 μ	-	-	19.1	537 GeV	537 GeV	1.05 TeV	1411.6795
GMSB, $\tilde{g} \rightarrow g\tilde{g}$, long-lived \tilde{g}	2 γ	-	-	20.3	440 GeV	440 GeV	1.05 TeV	1409.9542
GGM, $\tilde{g} \rightarrow g\tilde{g}$, long-lived \tilde{g}	displ. $\nu_e/\mu/\tau$	-	-	20.3	1.0 TeV	1.0 TeV	1.05 TeV	1504.05162
GGM, $\tilde{g} \rightarrow g\tilde{g}$, long-lived \tilde{g}	displ. $\nu_e/\mu/\tau$	-	-	20.3	1.0 TeV	1.0 TeV	1.05 TeV	1504.05162
RPV								
LFV $p\bar{p} \rightarrow X, Y, Z \rightarrow q\bar{q}/\ell\ell/\mu\tau$	$q\bar{q}/\mu\tau$	-	-	3.2	1.9 TeV	1.9 TeV	1.05 TeV	1607.08079
Bilinear RPV CMSM	2 μ jets (SS)	0-3 b	Yes	20.3	1.48 TeV	1.48 TeV	1.05 TeV	1404.2500
$\tilde{g}\tilde{g} \rightarrow g\tilde{g}$	4 μ jets	-	-	13.3	1.14 TeV	1.14 TeV	1.05 TeV	ATLAS-CONF-2016-075
$\tilde{g}\tilde{g} \rightarrow g\tilde{g}$	3 μ jets + τ	-	-	20.3	450 GeV	450 GeV	1.05 TeV	1405.5086
$\tilde{g}\tilde{g} \rightarrow g\tilde{g}$	0-4 large-R jets	-	-	14.8	1.08 TeV	1.08 TeV	1.05 TeV	ATLAS-CONF-2016-057
$\tilde{g}\tilde{g} \rightarrow g\tilde{g}$	0-4 large-R jets	-	-	14.8	1.55 TeV	1.55 TeV	1.05 TeV	ATLAS-CONF-2016-057
$\tilde{g}\tilde{g} \rightarrow g\tilde{g}$	1 μ , 8-10 jets/0-4 b	-	-	36.1	2.1 TeV	2.1 TeV	1.05 TeV	ATLAS-CONF-2017-013
$\tilde{g}\tilde{g} \rightarrow g\tilde{g}$	1 μ , 8-10 jets/0-4 b	-	-	36.1	1.65 TeV	1.65 TeV	1.05 TeV	ATLAS-CONF-2017-013
$\tilde{g}\tilde{g} \rightarrow g\tilde{g}$	2 jets + 2 b	-	-	15.4	410 GeV	450-510 GeV	1.05 TeV	ATLAS-CONF-2016-052, ATLAS-CONF-2016-084
$\tilde{g}\tilde{g} \rightarrow g\tilde{g}$	2 jets	-	-	20.3	6.4-1.0 TeV	6.4-1.0 TeV	1.05 TeV	ATLAS-CONF-2016-015
Other								
Scholar charm, $\tilde{g} \rightarrow g\tilde{g}$	0	2 μ	Yes	20.3	510 GeV	510 GeV	1.05 TeV	1501.01325

*Only a selection of the available mass limits on new states or phenomena is shown. Many of the limits are based on simplified models, c.f. refs. for the assumptions made.

ATLAS Preliminary

$\sqrt{s} = 7, 8, 13 \text{ TeV}$

ATLAS Exotics Searches* - 95% CL Exclusion

Status: August 2016

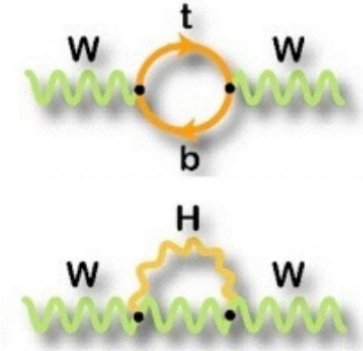
Model	ℓ, γ	Jets [†]	E_{miss}^T	$\int \mathcal{L} dt [fb^{-1}]$	Limit	Reference
Extra dimensions						
ADD $G_{KK} + g/\ell$	-	$\geq 1j$	Yes	3.2	M_{Pl} 6.56 TeV	n = 2
ADD non-resonant $\ell\ell$	2 μ	-	-	20.3	M_{Pl} 4.7 TeV	n = 3 HeZ
ADD OBH + g	1 μ	1j	-	20.3	M_{Pl} 5.2 TeV	n = 6
ADD OBH	2 μ	2j	-	15.7	M_{Pl} 8.7 TeV	n = 6
ADD BH Σ, π, τ	$\geq 1 \mu, \tau$	$\geq 2j$	-	3.2	M_{Pl} 8.2 TeV	n = 6, $M_{Pl} = 3 \text{ TeV}$, rot BH
ADD BH multiplet	-	$\geq 3j$	-	3.6	M_{Pl} 9.55 TeV	n = 6, $M_{Pl} = 3 \text{ TeV}$, rot BH
RS1 $G_{KK} \rightarrow \ell\ell$	2 μ	-	-	20.3	G_{KK} mass 2.68 TeV	$k/M_{Pl} = 0.1$
RS1 $G_{KK} \rightarrow \gamma\gamma$	2 γ	-	-	20.3	G_{KK} mass 3.2 TeV	$k/M_{Pl} = 0.1$
Bulk RS $G_{KK} \rightarrow WW \rightarrow q\bar{q}\ell$	1 μ, τ	1j	Yes	13.2	G_{KK} mass 1.24 TeV	$k/M_{Pl} = 1.0$
Bulk RS $G_{KK} \rightarrow HH \rightarrow b\bar{b}b\bar{b}$	1 μ, τ	4b	-	13.3	G_{KK} mass 360-860 GeV	$k/M_{Pl} = 1.0$
Bulk RS $R_{KK} \rightarrow t\bar{t}$	1 μ, τ	$\geq 2b, \geq 4j$	Yes	20.3	Box mass 2.2 TeV	BR = 0.925
ZUED / RPP	1 μ, τ	$\geq 2b, \geq 4j$	Yes	3.2	RK mass 1.46 TeV	Tier (1,1), BR($A^{(1)} \rightarrow t\bar{t}$) = 1
Gauge bosons						
SSM $Z' \rightarrow \ell\ell$	2 μ, τ	-	-	13.3	Z' mass 4.05 TeV	ATLAS-CONF-2016-045
SSM $Z' \rightarrow \tau\tau$	2 τ	-	-	19.5	Z' mass 2.62 TeV	1502.07177
Leptophobic $Z' \rightarrow b\bar{b}$	2 b	-	-	3.2	Z' mass 1.5 TeV	1603.08791
SSM $W' \rightarrow \ell\nu$	1 μ, τ	-	Yes	13.3	W' mass 4.74 TeV	ATLAS-CONF-2016-061
HVT $W' \rightarrow WZ \rightarrow qq\nu$ model A	0 μ, τ	1j	Yes	13.2	W' mass 2.4 TeV	ATLAS-CONF-2016-082
HVT $W' \rightarrow WZ \rightarrow qq\nu$ model B	0 μ, τ	2j	-	15.5	W' mass 3.0 TeV	ATLAS-CONF-2016-058
LRSM $W_{2,3} \rightarrow tb$	0 μ, τ	2b, 0-1j	Yes	20.3	W' mass 1.92 TeV	1410.4103
LRSM $W_{2,3} \rightarrow tb$	0 μ, τ	$\geq 1b, 1j$	Yes	20.3	W' mass 1.76 TeV	1406.0888
CI						
CI $e\bar{e} \rightarrow \mu\mu$	2 μ, τ	2j	-	15.7	A	ATLAS-CONF-2016-069
CI $e\bar{e} \rightarrow \mu\mu$	2 μ, τ	$\geq 1b, \geq 1j$	Yes	20.3	A	1607.08069
CI $e\bar{e} \rightarrow \mu\mu$	2(SS) $\geq 2 \mu, \tau \geq 1b, \geq 1j$	Yes	20.3	A	A	1504.04605
DM						
Axial-vector mediator (Dirac DM)	0 μ, τ	$\geq 1j$	Yes	3.2	m_A 1.0 TeV	1604.07773
Axial-vector mediator (Dirac DM)	0 μ, τ	1j	Yes	3.2	m_A 710 GeV	1604.01306
$ZZ_{\chi^{\pm}}$ EFT (Dirac DM)	0 μ, τ	1j, 5-1j	Yes	3.2	m_A 590 GeV	ATLAS-CONF-2015-080
LQ						
Scalar LQ 1 $^{\text{st}}$ gen	2 e, μ	$\geq 2j$	-	3.2	LQ mass 1.1 TeV	$\beta = 1$
Scalar LQ 2 $^{\text{nd}}$ gen	2 μ, τ	$\geq 2j$	-	3.2	LQ mass 1.05 TeV	$\beta = 1$
Scalar LQ 3 $^{\text{rd}}$ gen	1 μ, τ	$\geq 1b, \geq 3j$	Yes	20.3	LQ mass 640 GeV	$\beta = 0$
Heavy quarks						
VLO $T\bar{T} \rightarrow H\bar{H} + X$	1 μ, τ	$\geq 2b, \geq 3j$	Yes	20.3	T mass 855 GeV	T in (T \bar{T}) doublet
VLO $Y\bar{Y} \rightarrow W\bar{b} + X$	1 μ, τ	$\geq 1b, \geq 3j$	Yes	20.3	Y mass 770 GeV	Y in (B \bar{Y}) doublet
VLO $B\bar{B} \rightarrow H\bar{b} + X$	1 μ, τ	$\geq 2b, \geq 3j$	Yes	20.3	B mass 735 GeV	isospin singlet
VLO $B\bar{B} \rightarrow Z\bar{b} + X$	2 μ, τ	$\geq 2b, \geq 1j$	Yes	20.3	B mass 755 GeV	B in (B \bar{Y}) doublet
VLO $Q\bar{Q} \rightarrow W\bar{g}W\bar{g}$	1 μ, τ	2j	Yes	20.3	Q mass 690 GeV	1509.04261
VLO $T_{3,1} \bar{T}_{3,1} \rightarrow W\bar{W}W\bar{W}$	2(SS) $\geq 2 \mu, \tau \geq 1b, \geq 1j$	Yes	20.3	$T_{3,1}$ mass 990 GeV	ATLAS-CONF-2016-032	
Excited fermions						
Excited quark $q^* \rightarrow q\gamma$	1 γ	1j	-	3.2	q^* mass 4.4 TeV	only u^* and d^* , $A = m(q^*)$
Excited quark $q^* \rightarrow g\bar{g}$	-	2j	-	15.7	q^* mass 5.6 TeV	only u^* and d^* , $A = m(q^*)$
Excited quark $q^* \rightarrow b\bar{g}$	-	1b, 1j	-	8.8	q^* mass 2.3 TeV	$A = 3.0 \text{ TeV}$
Excited quark $q^* \rightarrow W\bar{e}$	1 or 2 e, μ, τ	1b, 2-0j	-	20.3	q^* mass 1.5 TeV	$f_u = f_d = f_e = 1$

W mass measurement

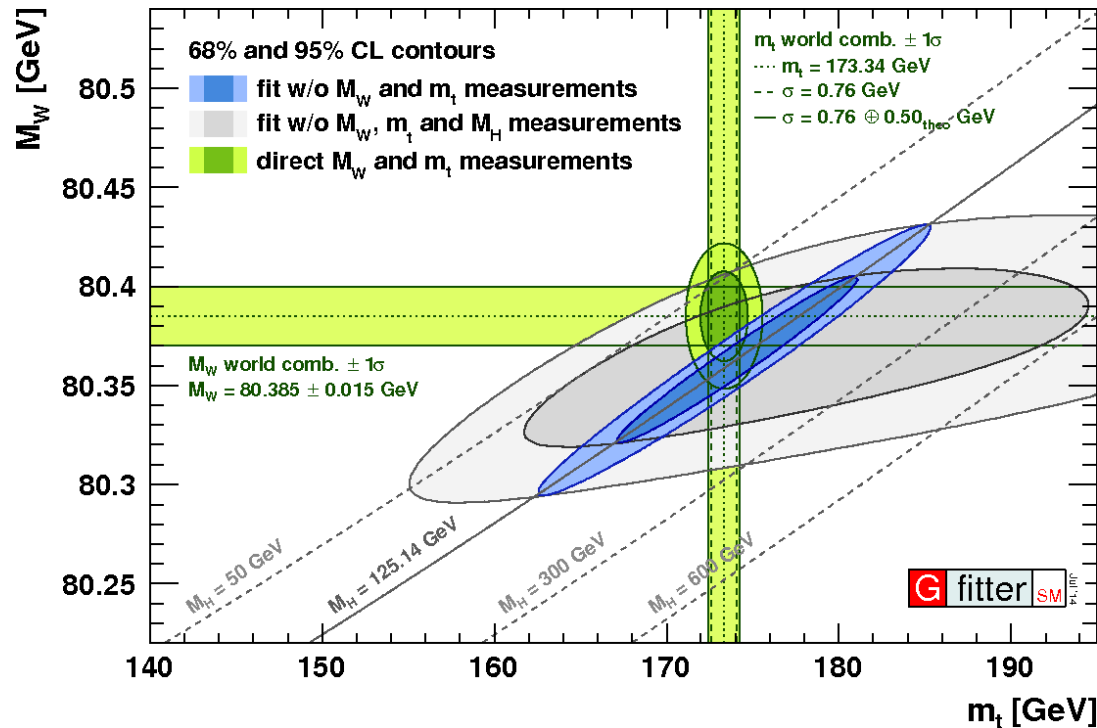
In the electroweak sector of the SM, the W mass at the loop level:

$$m_W^2 \left(1 - \frac{m_W^2}{m_Z^2} \right) = \frac{\pi\alpha}{\sqrt{2}G_F} (1 + \Delta r)$$

In SM, Δr reflects loop corrections and depends on m_t^2 and $\ln m_H$



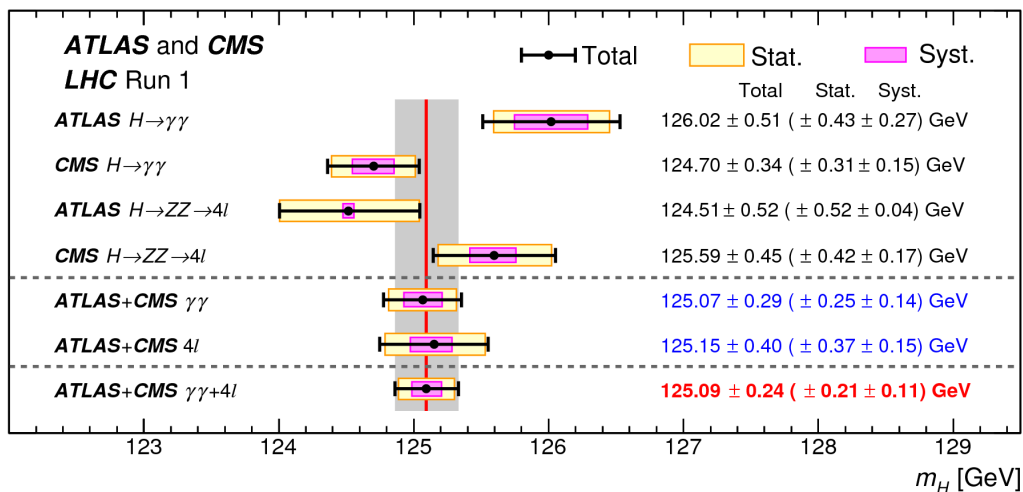
The relation between M_W , m_t , and M_H provides stringent test of the SM and is sensitive to new Physics



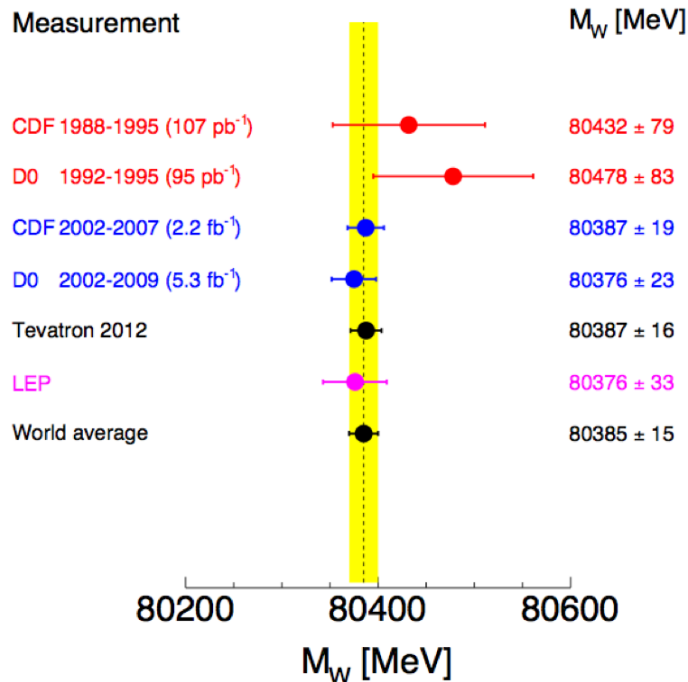
Status of the measurements

Higgs mass

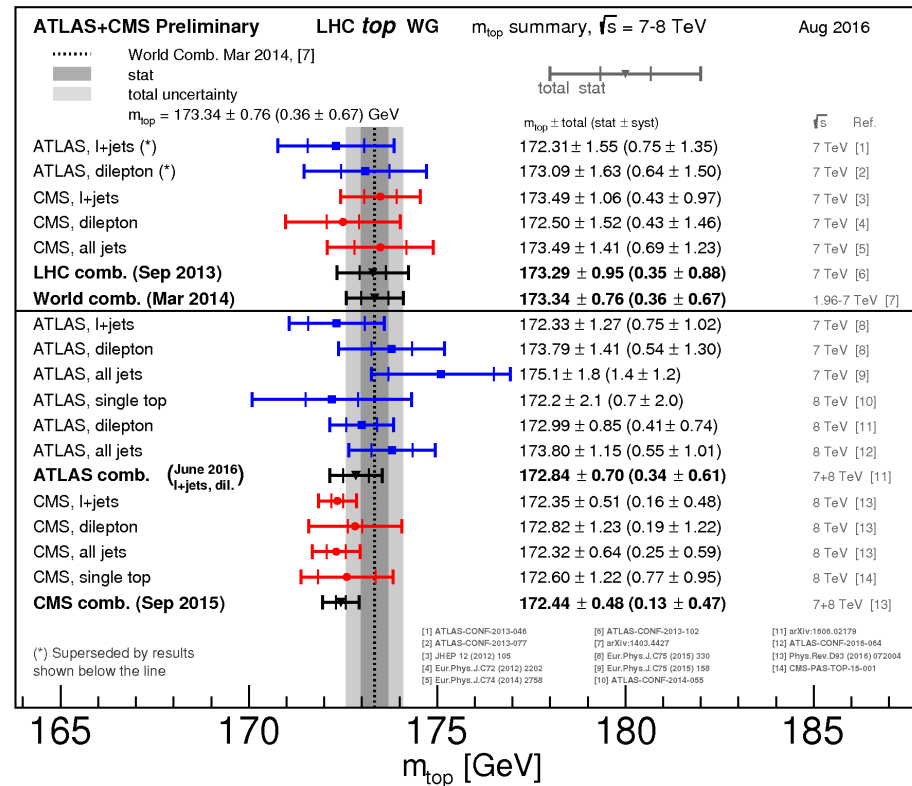
Phys. Rev. Lett. 114, 191803



Mass of the W Boson



Top mass



W mass

LEP+Tevatron: M_W uncertainty ~ 15 MeV
 Best individual measurement:
 CDF M_W uncertainty 19 MeV

Tevatron results

CDF experiment:

[Phys. Rev. Lett.108 \(2012\) 151803](#)

electron/muon channels
2.2 fb⁻¹ integrated luminosity

$$m_W = 80387 \pm 12(\text{stat}) \pm 15(\text{syst}) \text{ MeV}$$

Source	Uncertainty (MeV)
Lepton energy scale and resolution	7
Recoil energy scale and resolution	6
Lepton removal	2
Backgrounds	3
$p_T(W)$ model	5
Parton distributions	10
QED radiation	4
W -boson statistics	12
Total	19

D0 experiment:

[Phys. Rev. Lett. 108 \(2012\) 151804](#)

electron channel
~5.3 fb⁻¹ integrated luminosity

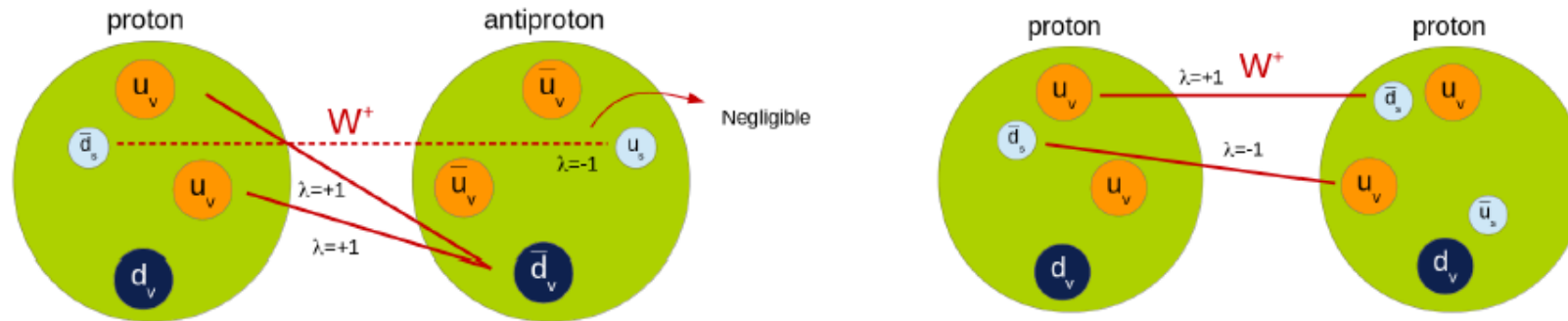
$$m_W = 80375 \pm 11(\text{stat}) \pm 20(\text{syst}) \text{ MeV}$$

Source	ΔM_W (MeV)		
	m_T	p_T^e	E_T
Electron energy calibration	16	17	16
Electron resolution model	2	2	3
Electron shower modeling	4	6	7
Electron energy loss model	4	4	4
Hadronic recoil model	5	6	14
Electron efficiencies	1	3	5
Backgrounds	2	2	2
Experimental subtotal	18	20	24
PDF	11	11	14
QED	7	7	9
Boson p_T	2	5	2
Production subtotal	13	14	17
Total	22	24	29

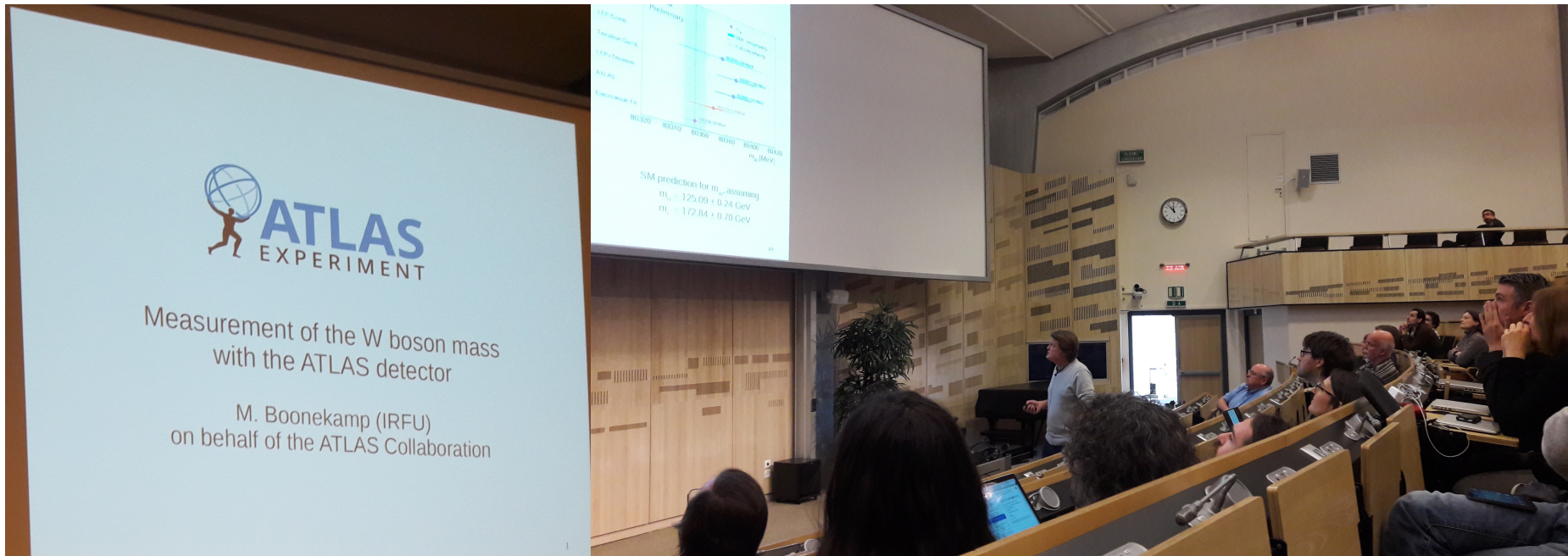
$$M_W = 80387 \pm 16 \text{ MeV}$$

W mass @ LHC

Challenging environment @LHC: pileup, need a high experimental precision and an accurate theoretical modelling



- W^+/W^- production is asymmetric \rightarrow charge-dependent analysis
- Second generation quark PDFs play a larger role at the LHC (25% of the W -boson production is induced by at least one second generation quark s or c).
- The W polarisation is determined by the difference between the u , d valence and sea densities



CERN Courier January/February 2017

News

LHC EXPERIMENTS

ATLAS makes precision measurement of W mass

arXiv.org > hep-ex > arXiv:1701.07240v1

arXiv:1701.07240 [hep-ex]

Search (Help | A)

High Energy Physics - Experiment

Measurement of the W -boson mass in pp collisions at $\sqrt{s} = 7$ TeV with the ATLAS detector

ATLAS Collaboration

(Submitted on 25 Jan 2017)

paper is submitted to EPJC



Strategy of the measurement (I)

Not possible to fully reconstruct W mass

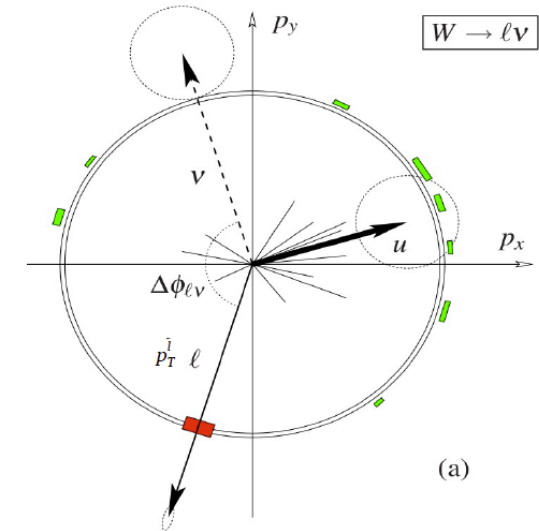
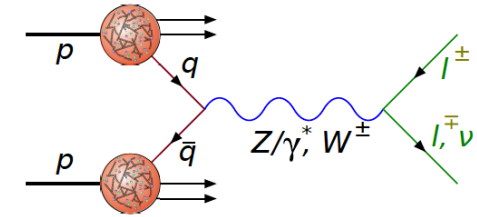
Sensitive final state distributions: p_T^ℓ , m_T , $p_T^{\text{miss}*}$

$$\vec{p}_T^{\text{miss}} = -(\vec{p}_T^\ell + \vec{u}_T) \quad m_T = \sqrt{2p_T^\ell p_T^{\text{miss}} (1 - \cos \Delta\phi)}$$

u_T being the **recoil**

In W, Z events $-u_T$ provides an estimate of the boson p_T

Categories for the measurement:



Decay channel	$W \rightarrow e\nu$	$W \rightarrow \mu\nu$
Kinematic distributions	p_T^ℓ, m_T	p_T^ℓ, m_T
Charge categories	W^+, W^-	W^+, W^-
$ \eta_\ell $ categories	$[0, 0.6], [0.6, 1.2], [1.8, 2.4]$	$[0, 0.8], [0.8, 1.4], [1.4, 2.0], [2.0, 2.4]$

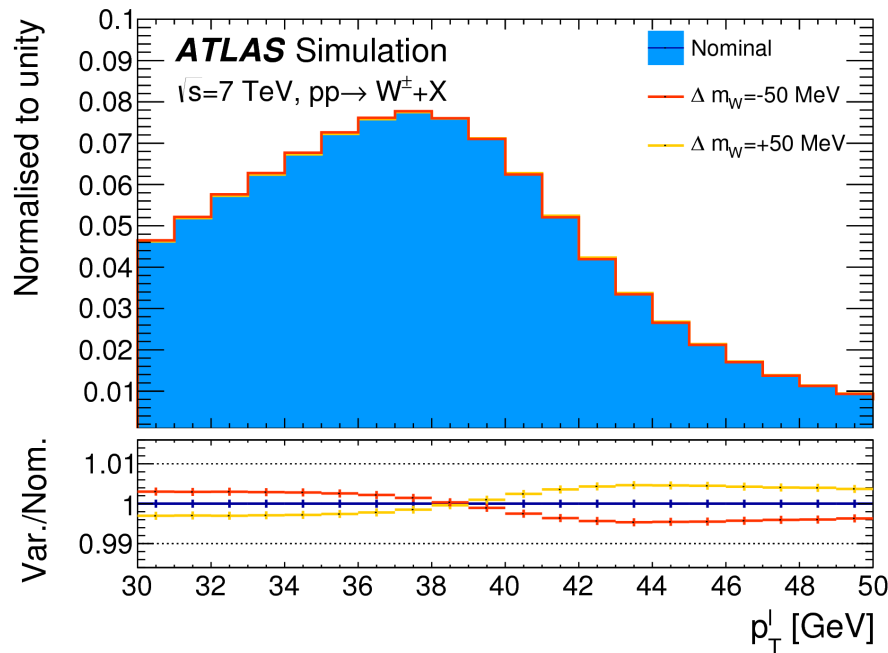
*used as cross-check only

Strategy of the measurement (II)

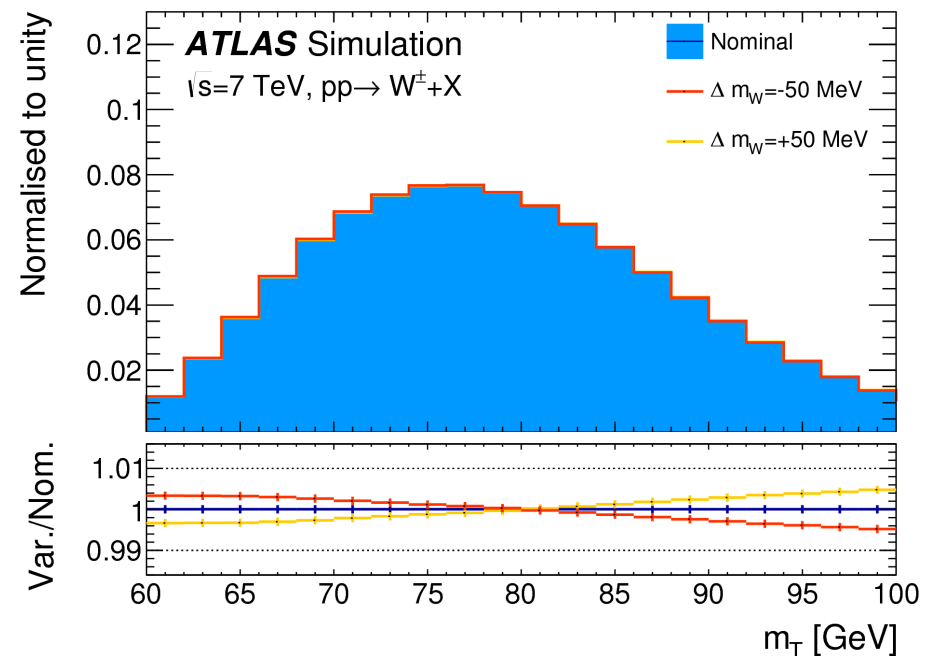
Template fit approach: compute the p_T^\perp and m_T distributions for different assumed values of m_W^* \rightarrow χ^2 minimisation gives the best fit template.

Predictions for different m_W values are obtained by reweighting the boson invariant mass distribution according to the BW parameterisation.

$$\frac{d\sigma}{dm} \propto \frac{m^2}{(m^2 - m_V^2)^2 + m^4 \Gamma_V^2 / m_V^2}$$



p_T^\perp has a Jacobian edge at $m_W/2$



m_T has a Jacobian edge at m_W

* *A blinding offset* was applied throughout the measurement and removed when consistent results were found.

Selection cuts

Lepton selections:

- muons isolated (track-based) $|\eta| < 2.4$
- electrons isolated (track+calorimeter-based) tight identified $0 < |\eta| < 1.2$, $1.8 < |\eta| < 2.4$

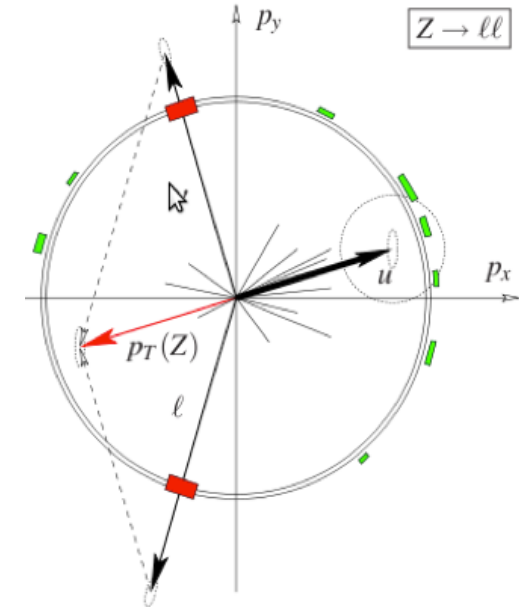
Kinematic requirements: $p_T^l > 30$ GeV, $m_T > 60$ GeV, $MET > 30$ GeV and $\text{recoil}(u_T) < 30$ GeV

~6M/8M observed in the electron/muon channel

$ \eta_l $ range	0–0.8	0.8–1.4	1.4–2.0	2.0–2.4	Inclusive
$W^+ \rightarrow \mu^+ \nu$	1 283 332	1 063 131	1 377 773	885 582	4 609 818
$W^- \rightarrow \mu^- \bar{\nu}$	1 001 592	769 876	916 163	547 329	3 234 960
$ \eta_l $ range	0–0.6	0.6–1.2		1.8–2.4	Inclusive
$W^+ \rightarrow e^+ \nu$	1 233 960	1 207 136		956 620	3 397 716
$W^- \rightarrow e^- \bar{\nu}$	969 170	908 327		610 028	2 487 525

Z-boson sample

Benefit from the fully reconstructed mass in **Z-boson sample** to validate the analysis and to provide significant **experimental** (*lepton and recoil calibration using resp. m_Z measured at LEP and expected momentum balance with $p_T^{\ell\ell}$*) and **theoretical constraints** (*ancilliary measurements*).



The whole analysis is checked by performing **a measurement of the Z-boson mass** and comparing to the LEP value, also a cross-check Z mass measurement in “W-like” i.e removing the 2nd lepton and treating it like a neutrino

A similar W-like analysis was also done by CMS **CMS PAS SMP-14-007**

Need to consider **additional** systematics for W mass measurement (*theory uncertainties, Z→W extrapolation and background*)



Experimental precision

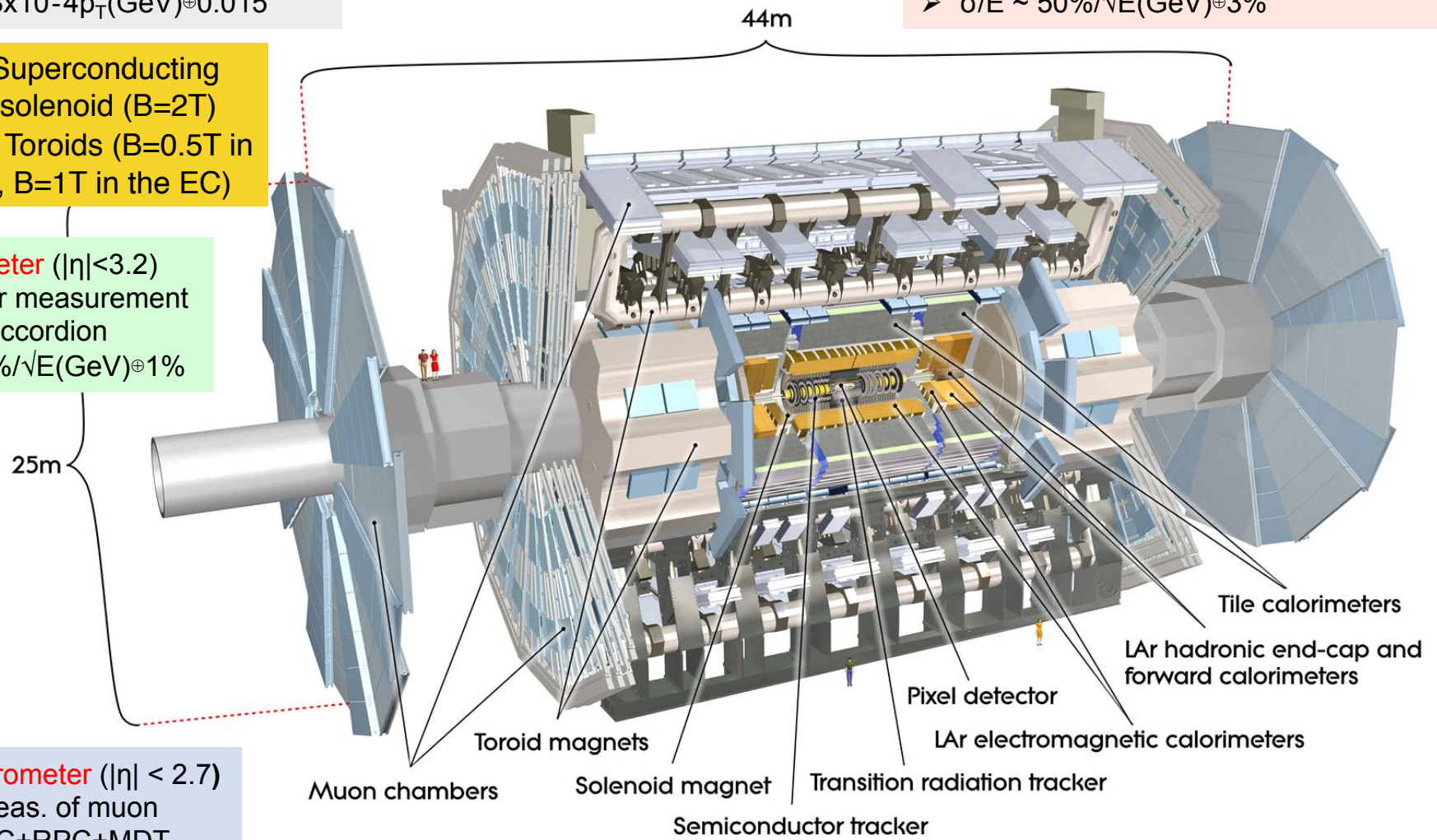
ATLAS detector

Inner detector ($|\eta| < 2.5$, $B=2T$)
 Tracking, vertexing, dE/dx , e/π ID
 ➤ Si pixels, Si strips, Trans. Rad. det.
 ➤ $\sigma/p_T \sim 3.8 \times 10^{-4} p_T(\text{GeV}) \oplus 0.015$

4 Magnets Superconducting
 • 1 Central solenoid ($B=2T$)
 • 3 Air core Toroids ($B=0.5T$ in the barrel, $B=1T$ in the EC)

EM Calorimeter ($|\eta| < 3.2$)
 e/γ ID trigger measurement
 ➤ Pb-Lar accordion
 ➤ $\sigma/E \sim 10\%/\sqrt{E(\text{GeV})} \oplus 1\%$

Hadron Calorimeter ($|\eta| < 5$)
 Trigger and meas. of jet/Emiss
 ➤ Fe/scintillator (central), Cu/W-LAr (fwd)
 ➤ $\sigma/E \sim 50\%/\sqrt{E(\text{GeV})} \oplus 3\%$



Muon spectrometer ($|\eta| < 2.7$)
 Trigger & meas. of muon
 ➤ CSC+TGC+RPC+MDT
 ➤ $\sigma/p_T < 10\%$ up to 1 TeV

Muon Calibration & Efficiency

Muon identified using combined ID+MS tracks, momentum measurement from ID only.

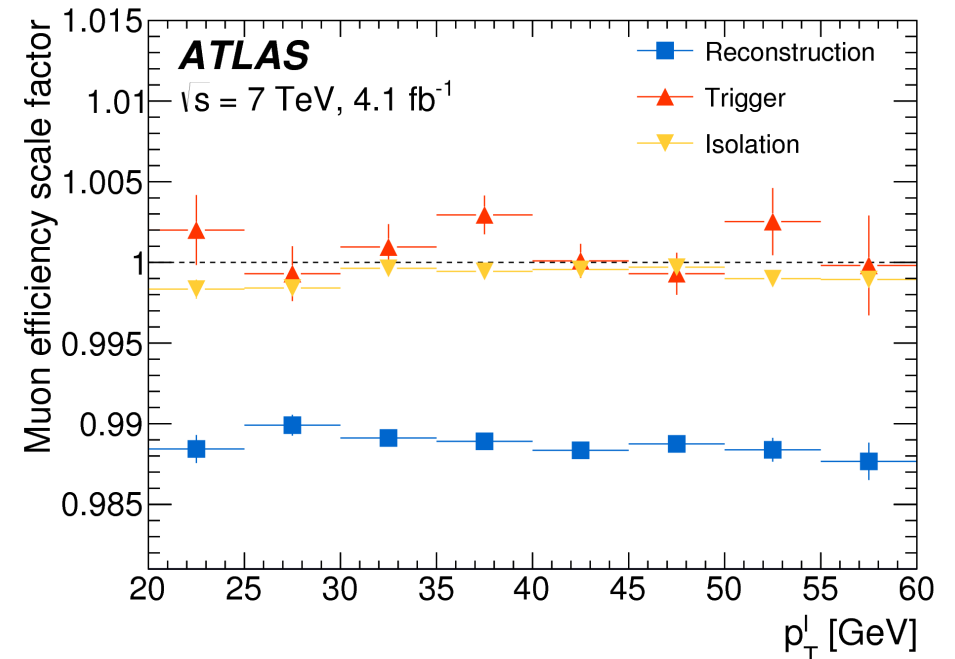
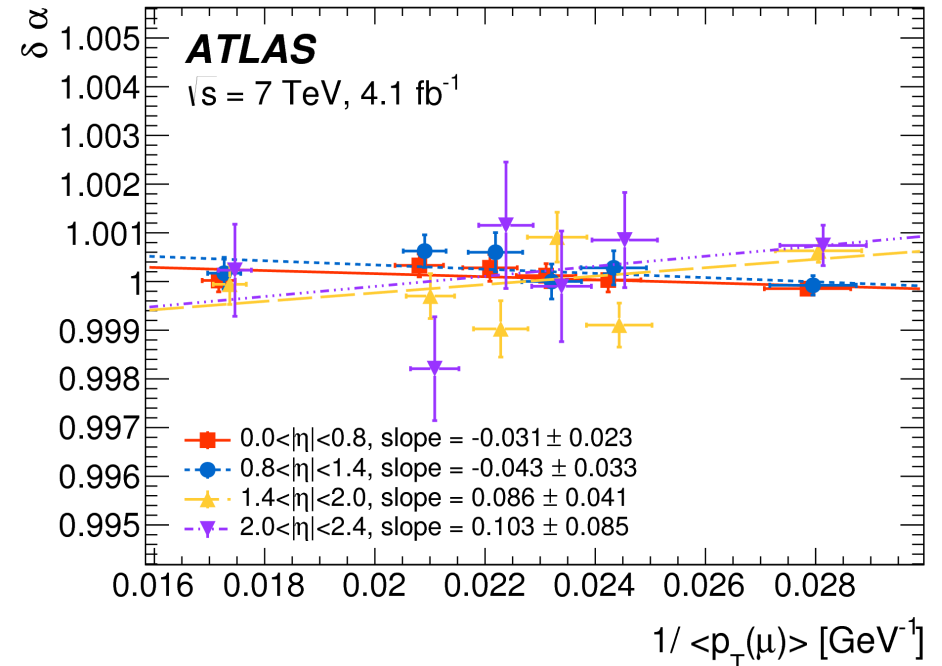
Calibration factors for ID-only muons derived from $Z \rightarrow \mu\mu$ and **sagitta bias** charge-dependent corrections from $Z \rightarrow \mu\mu$ and E/p of $W \rightarrow e\nu$. [Eur.Phys.J.C 74 \(2014\) 3130](#)

$$p_T^{\text{MC,corr}} = p_T^{\text{MC}} \times [1 + \alpha(\eta, \phi)] \times [1 + \beta_{\text{curv}}(\eta) \cdot G(0, 1) \cdot p_T^{\text{MC}}]$$

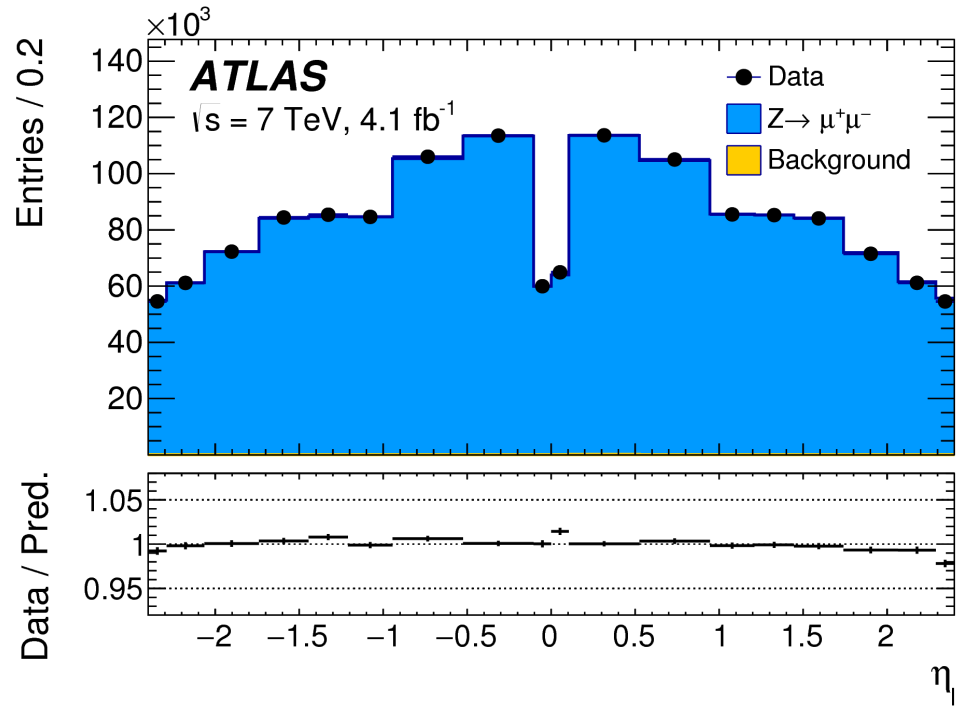
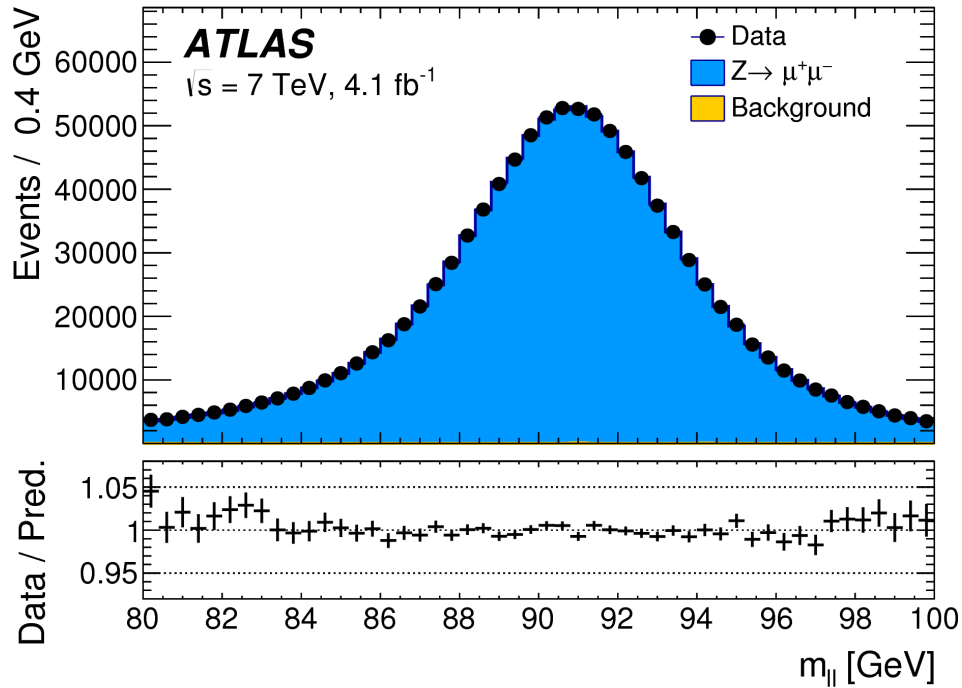
$$p_T^{\text{data,corr}} = \frac{p_T^{\text{data}}}{1 + q \cdot \delta(\eta, \phi) \cdot p_T^{\text{data}}}$$

Muon **trigger/id/iso efficiency** corrections data/MC evaluated in bins of p_T^l , η and charge.

Dominant uncertainty is the statistical uncertainty of the Z sample.



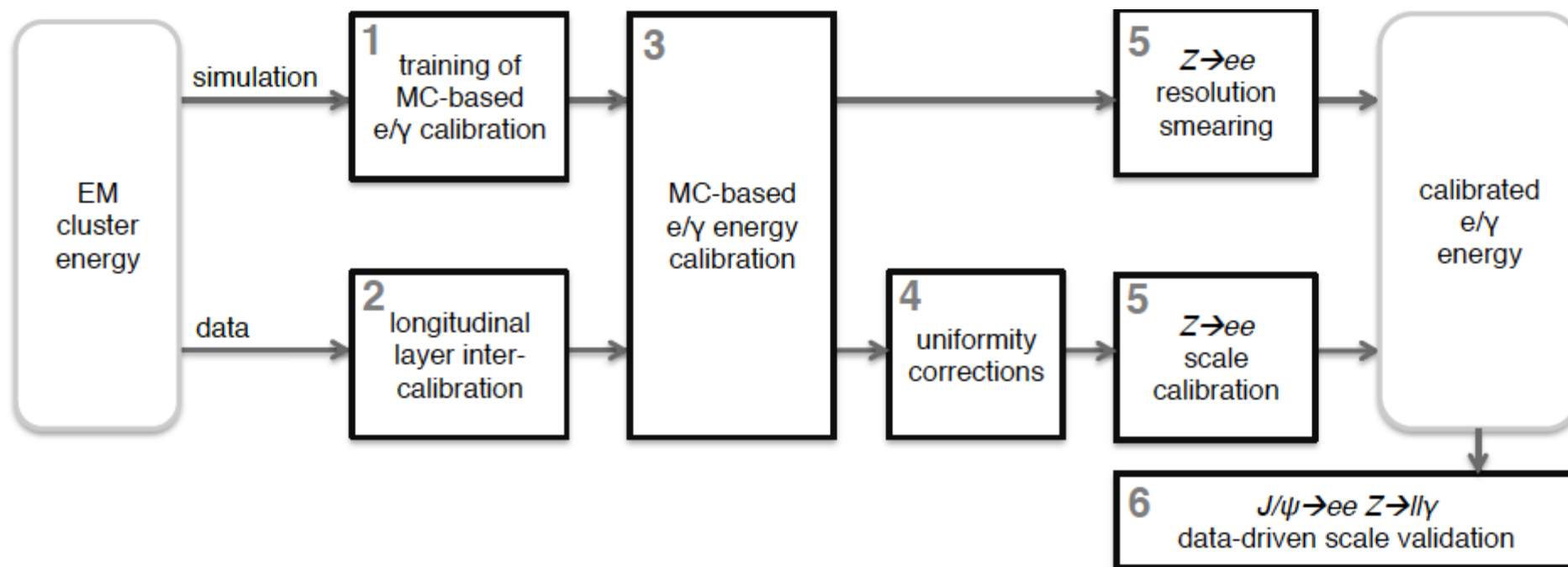
Muon Calibration & Efficiency



$ \eta_e $ range	[0.0, 0.8]		[0.8, 1.4]		[1.4, 2.0]		[2.0, 2.4]		Combined	
	p_T^l	m_T	p_T^l	m_T	p_T^l	m_T	p_T^l	m_T	p_T^l	m_T
Kinematic distribution										
δm_W [MeV]										
Momentum scale	8.9	9.3	14.2	15.6	27.4	29.2	111.0	115.4	8.4	8.8
Momentum resolution	1.8	2.0	1.9	1.7	1.5	2.2	3.4	3.8	1.0	1.2
Sagitta bias	0.7	0.8	1.7	1.7	3.1	3.1	4.5	4.3	0.6	0.6
Reconstruction and isolation efficiencies	4.0	3.6	5.1	3.7	4.7	3.5	6.4	5.5	2.7	2.2
Trigger efficiency	5.6	5.0	7.1	5.0	11.8	9.1	12.1	9.9	4.1	3.2
Total	11.4	11.4	16.9	17.0	30.4	31.0	112.0	116.1	9.8	9.7

Electron Calibration & Efficiency

Calibration for electrons closely follows the Run I calibration paper [Eur.Phys.J.C 74 \(2014\) 3071](#)



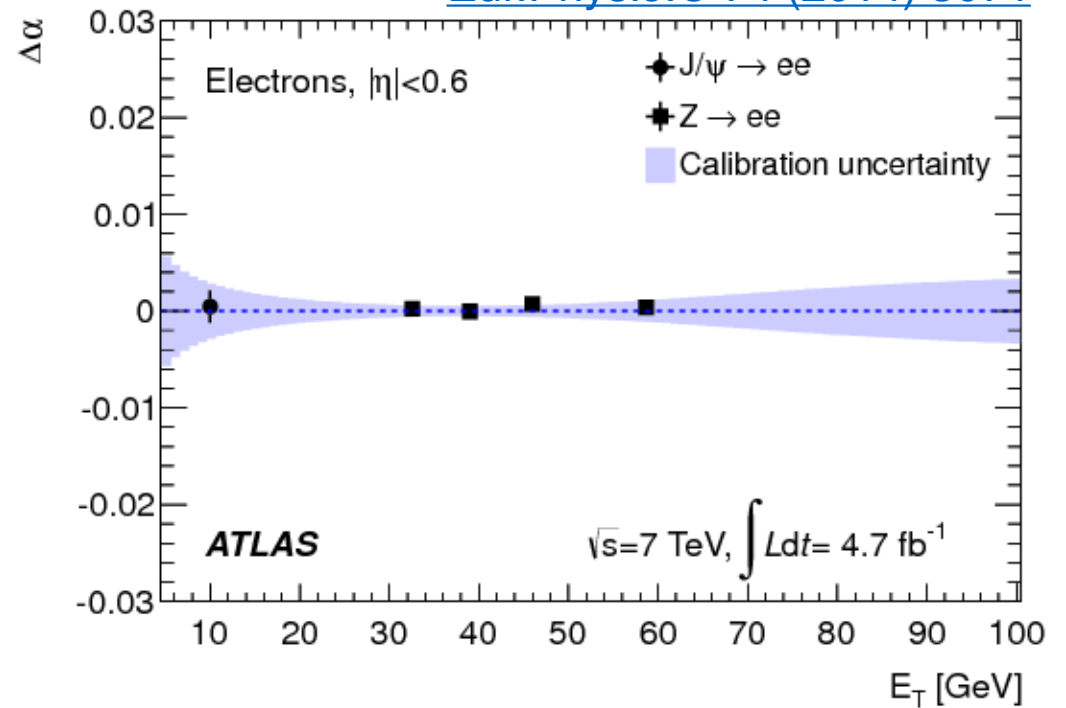
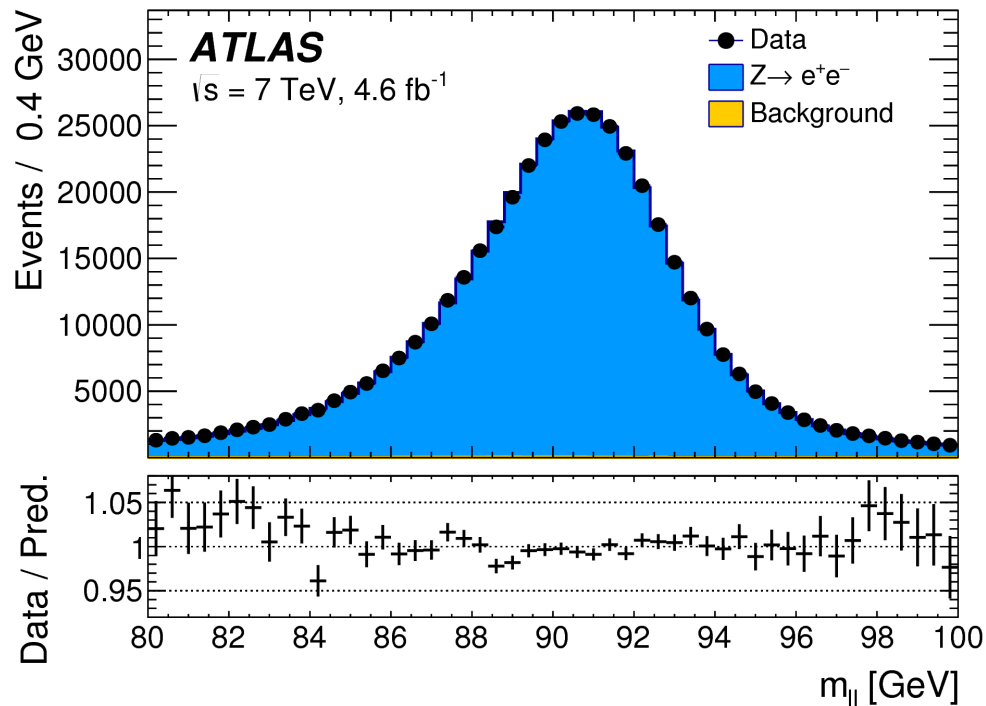
Exclude bin $1.2 < |\eta| < 1.82$ for the W mass measurement as the amount of passive material in front of the calorimeter and its uncertainty are largest in this region.

Azimuthal correction from $\langle E/p \rangle$ vs φ

Electron efficiency corrections as a function of η and p_T [Eur.Phys.J.C 74 \(2014\) 2941](#)

Electron Calibration & Efficiency

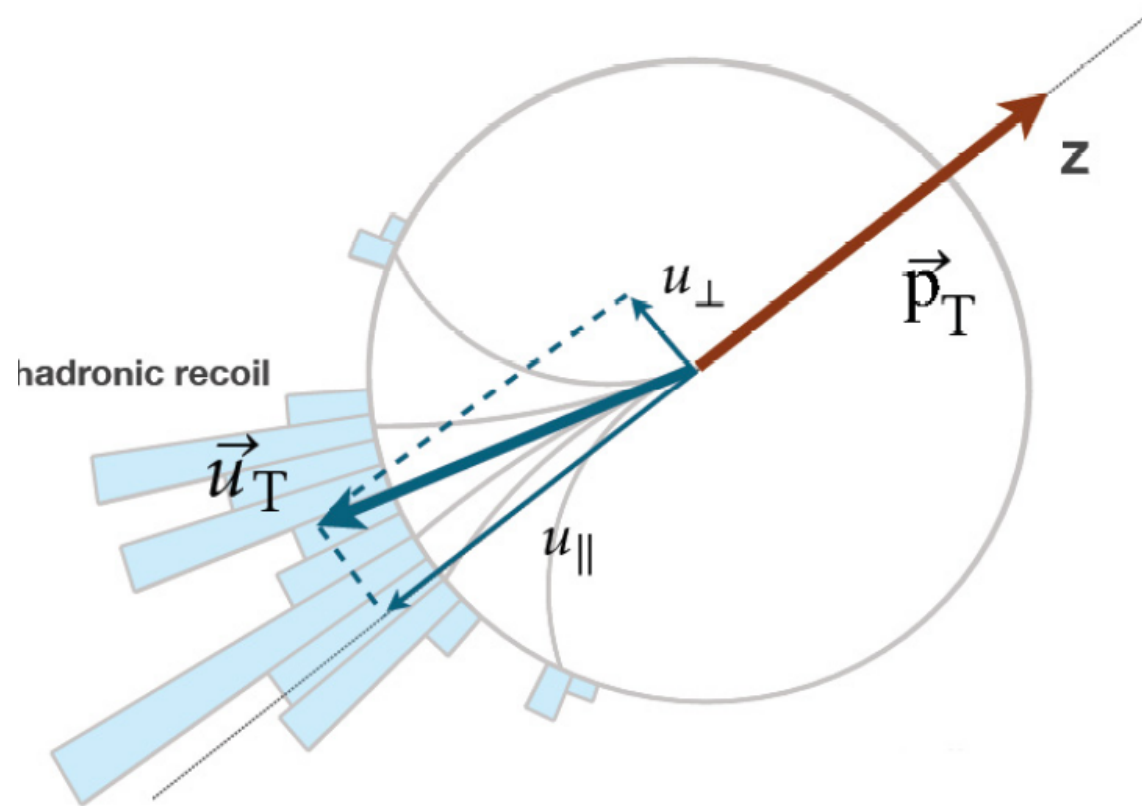
Eur.Phys.J.C 74 (2014) 3071



$ \eta_e $ range	[0.0, 0.6]		[0.6, 1.2]		[1.82, 2.4]		Combined	
Kinematic distribution	p_T^ℓ	m_T	p_T^ℓ	m_T	p_T^ℓ	m_T	p_T^ℓ	m_T
δm_W [MeV]								
Energy scale	10.4	10.3	10.8	10.1	16.1	17.1	8.1	8.0
Energy resolution	5.0	6.0	7.3	6.7	10.4	15.5	3.5	5.5
Energy linearity	2.2	4.2	5.8	8.9	8.6	10.6	3.4	5.5
Energy tails	2.3	3.3	2.3	3.3	2.3	3.3	2.3	3.3
Reconstruction efficiency	10.5	8.8	9.9	7.8	14.5	11.0	7.2	6.0
Identification efficiency	10.4	7.7	11.7	8.8	16.7	12.1	7.3	5.6
Trigger and isolation efficiencies	0.2	0.5	0.3	0.5	2.0	2.2	0.8	0.9
Charge mismeasurement	0.2	0.2	0.2	0.2	1.5	1.5	0.1	0.1
Total	19.0	17.5	21.1	19.4	30.7	30.5	14.2	14.3

Recoil Reconstruction

Vector sum of the momenta of all clusters measured in the calorimeters

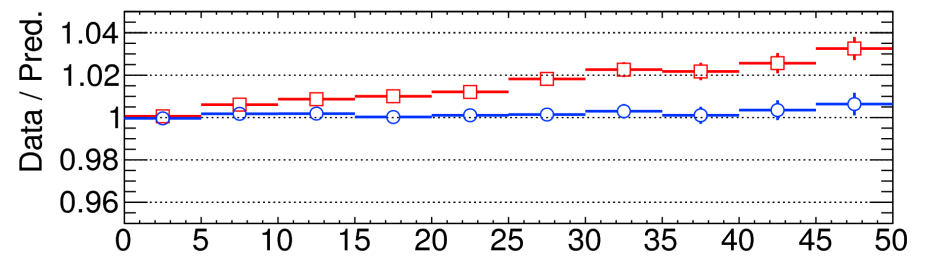
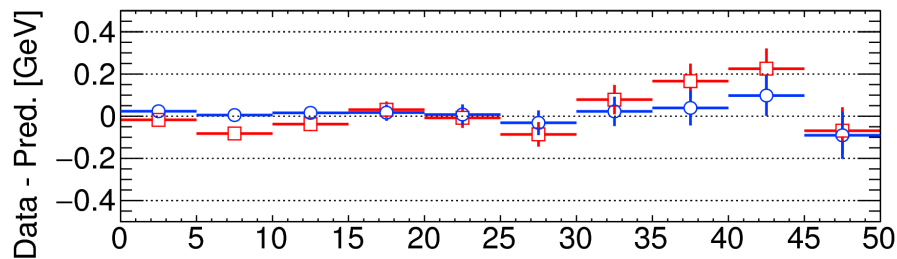
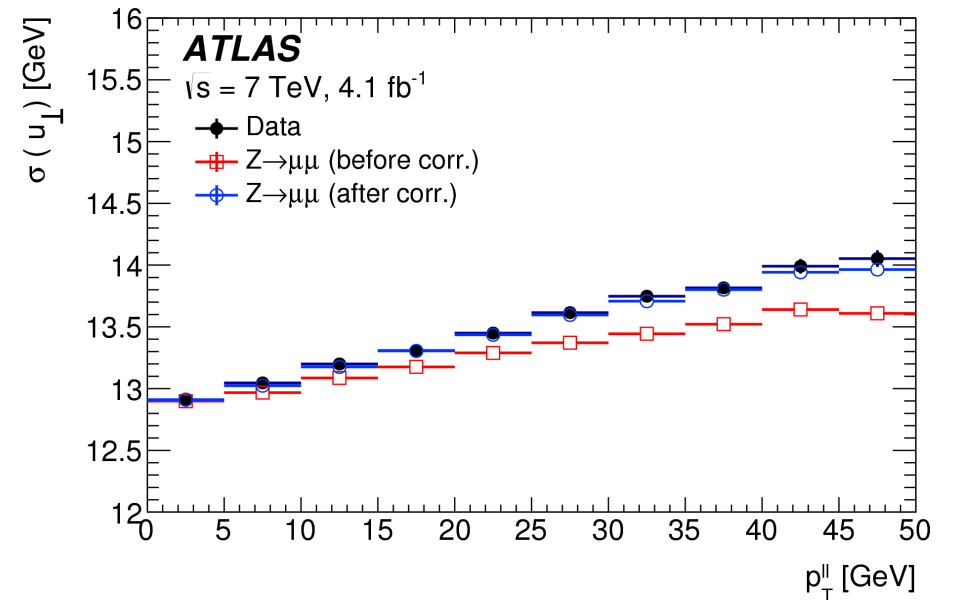
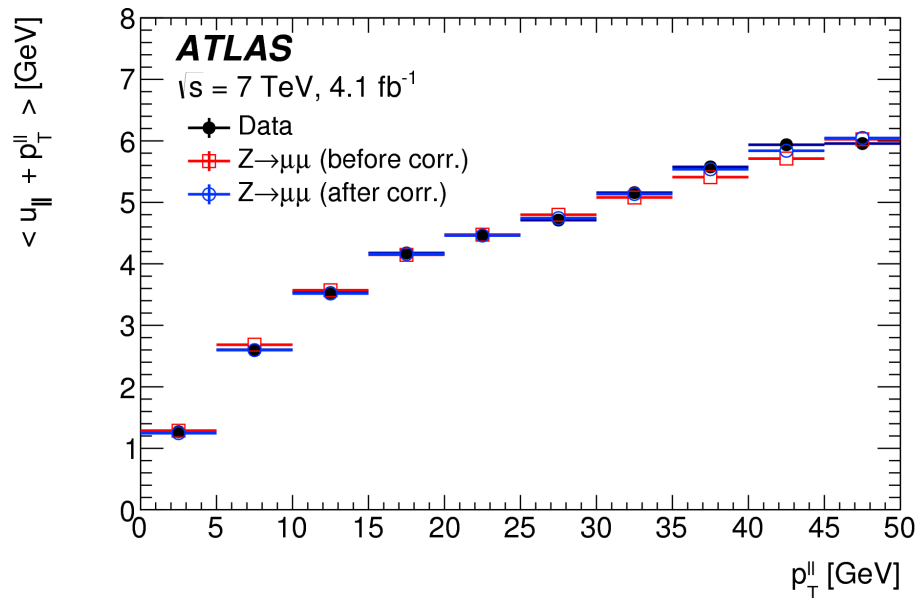


Also : u_{\parallel} is the projection of the recoil along the W decay lepton direction

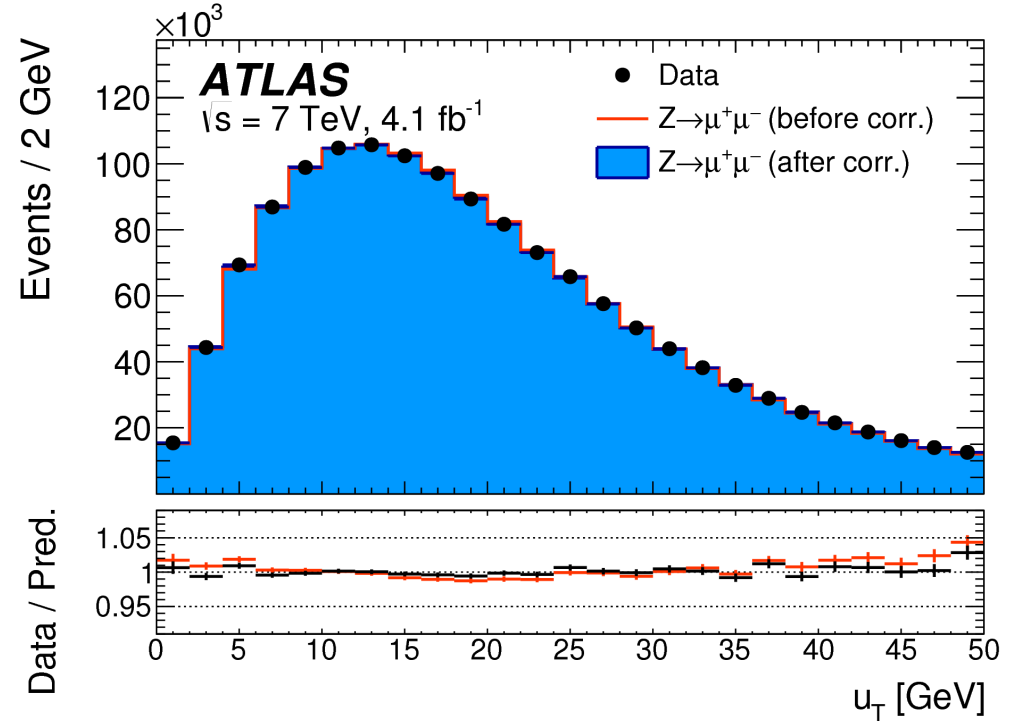
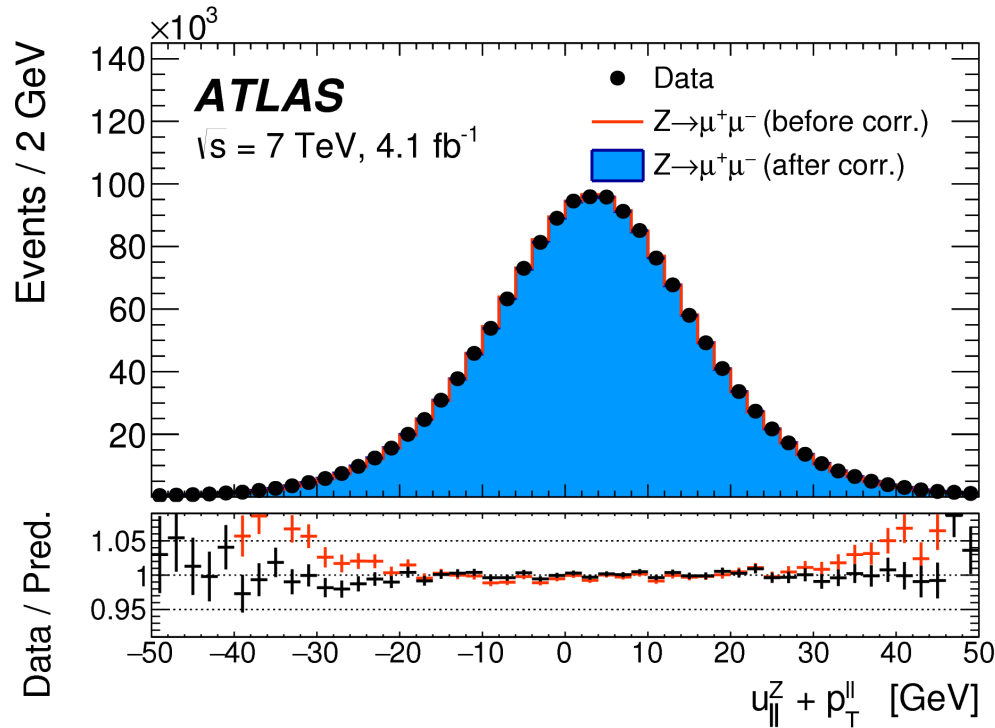
Recoil Calibration

Calibrate the scale (resolution) of the recoil using u_{\parallel} (u_{\perp}) from Z events

70-80% recoil response, remaining pileup dependence of the recoil resolution cluster-based.

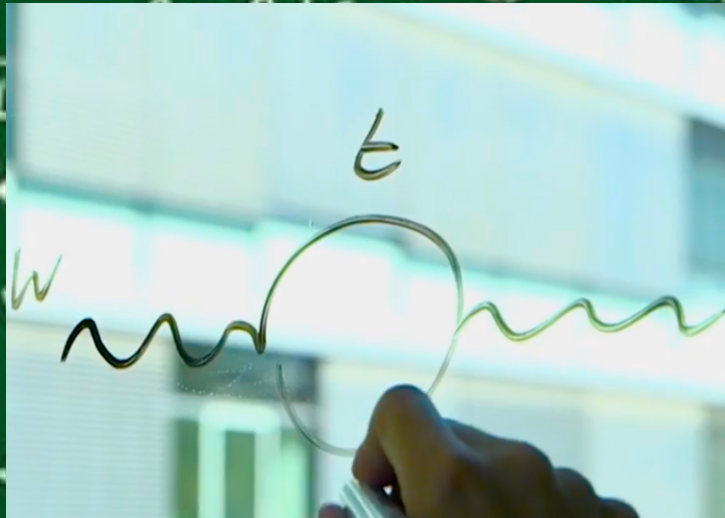


Recoil Calibration



	W^+		W^-		Combined	
	p_T^l	m_T	p_T^l	m_T	p_T^l	m_T
δm_W [MeV]						
$\langle \mu \rangle$ scale factor	0.2	1.0	0.2	1.0	0.2	1.0
$\Sigma \vec{E}_T$ correction	0.9	12.2	1.1	10.2	1.0	11.2
Residual corrections (statistics)	2.0	2.7	2.0	2.7	2.0	2.7
Residual corrections (interpolation)	1.4	3.1	1.4	3.1	1.4	3.1
Residual corrections ($Z \rightarrow W$ extrapolation)	0.2	5.8	0.2	4.3	0.2	5.1
Total	2.6	14.2	2.7	11.8	2.6	13.0

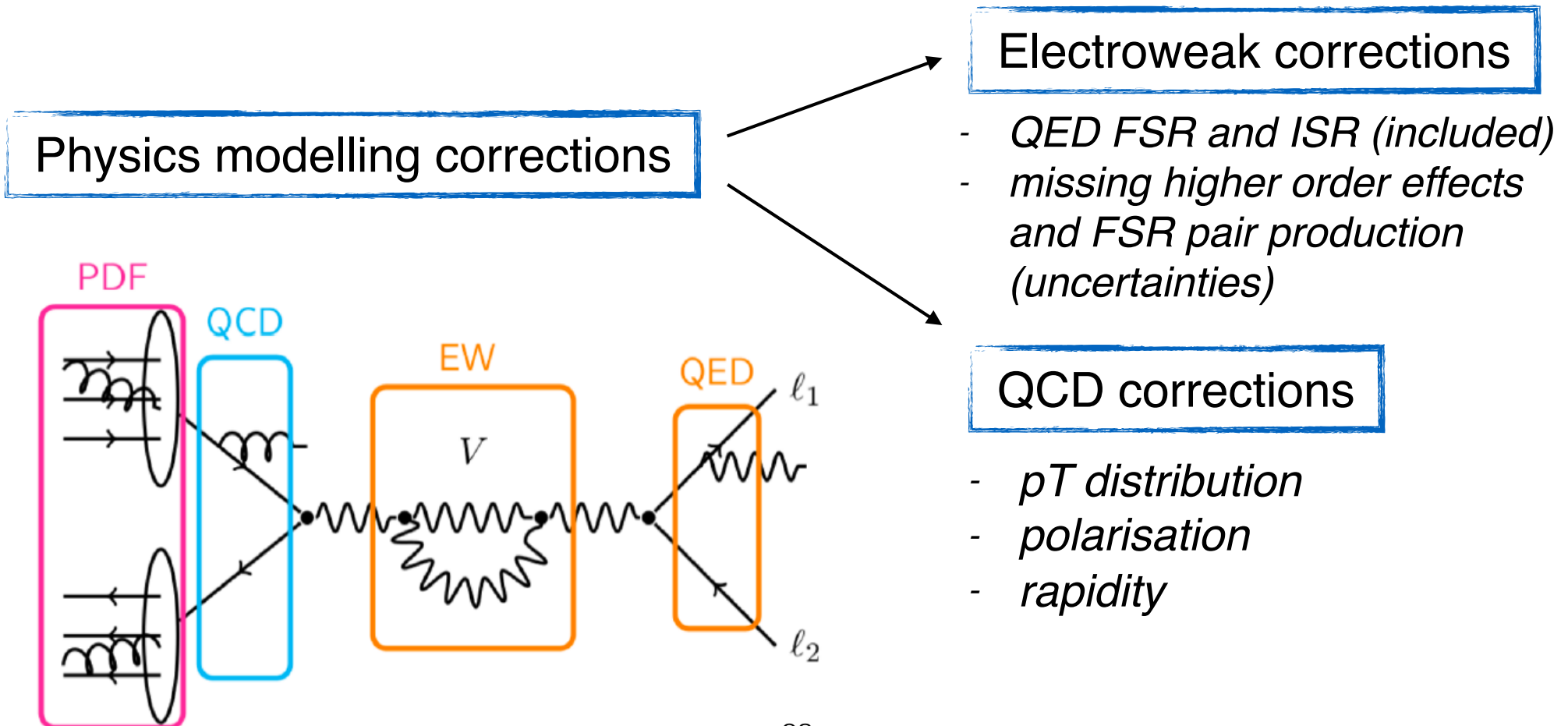
Physics modelling



Physics Modelling

No single generator able to describe all observed distributions.

Start from the Powheg+Pythia8 and apply corrections. Use ancillary measurements of Drell-Yan processes to validate (and tune) the model and assess systematic uncertainties.



EW corrections

QED effects: **FSR** (*dominant correction*) included in the simulation with PHOTOS, negligible uncertainty. QED **ISR** included through Pythia8 parton shower.

NLO EW effects: taken as uncertainties, **pure weak corrections** evaluated in the presence of QCD corrections, estimated using Winhac. **ISR-FSR interference**.

FSR **lepton pair production** estimated and added as an uncertainty. Formally higher order correction but a significant additional source of energy loss.

Decay channel	$W \rightarrow e\nu$		$W \rightarrow \mu\nu$	
	p_T^ℓ	m_T	p_T^ℓ	m_T
δm_W [MeV]				
FSR (real)	< 0.1	< 0.1	< 0.1	< 0.1
Pure weak and IFI corrections	3.3	2.5	3.5	2.5
FSR (pair production)	3.6	0.8	4.4	0.8
Total	4.9	2.6	5.6	2.6

QCD corrections

The Drell-Yan cross-section can be decomposed by **factorising** the dynamic of the boson production and the kinematic of the boson decay.

An approximate decomposition is given by:

$$\frac{d\sigma}{dp_1 dp_2} = \left[\frac{d\sigma(m)}{dm} \right] \left[\frac{d\sigma(y)}{dy} \right] \left[\frac{d\sigma(p_T, y)}{dp_T dy} \left(\frac{d\sigma(y)}{dy} \right)^{-1} \right] \left[(1 + \cos^2 \theta) + \sum_{i=0}^7 A_i(p_T, y) P_i(\cos \theta, \phi) \right]$$

Breit-Wigner

NNLO pQCD

Parton Shower

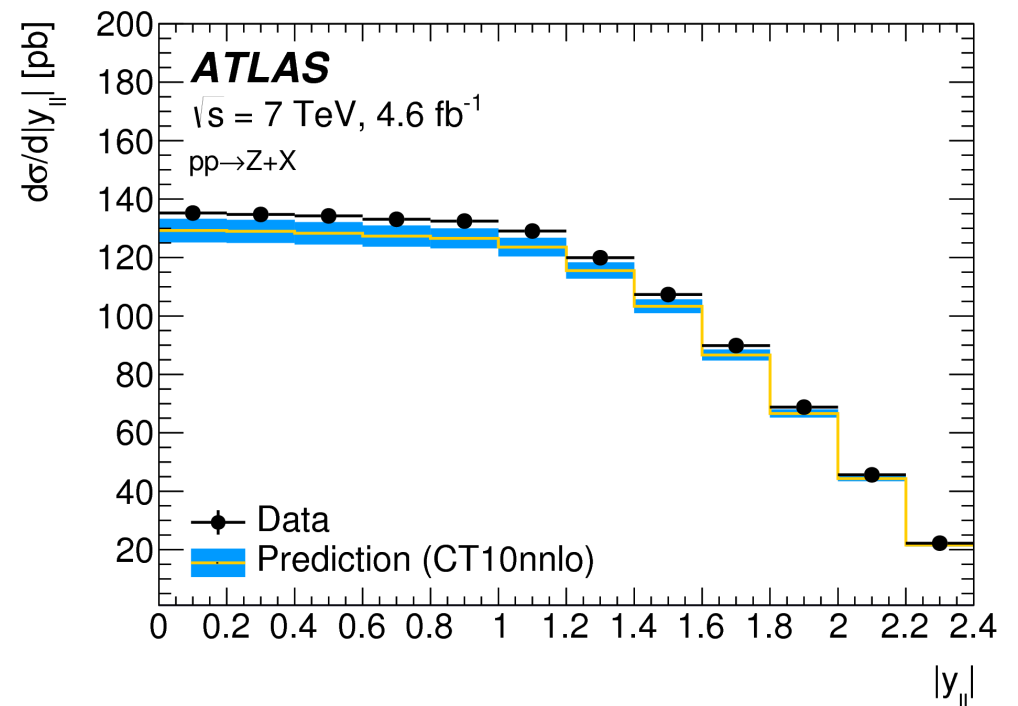
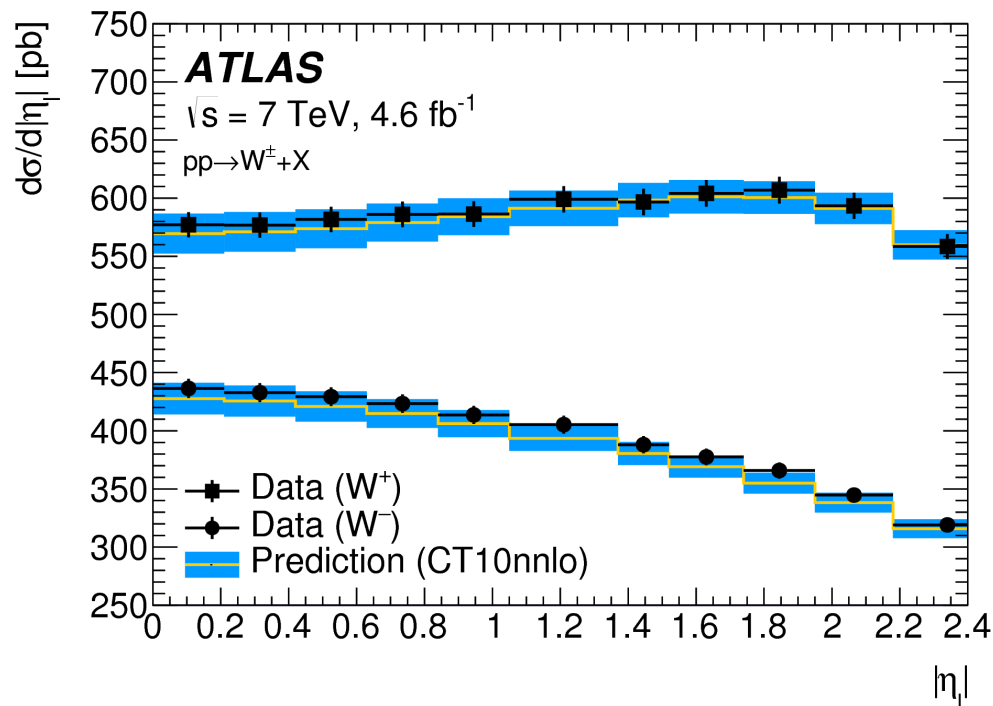
$d\sigma/dm$ is modelled with a BW parameterisation (+ EW corrections)

$d\sigma/dy$ and the A_i coefficients are modelled with fixed order pQCD at NNLO

$d\sigma/dp_T$ is modelled with parton shower (tried analytic resummation)

Rapidity distribution

The **rapidity distribution** is modelled with NNLO predictions and the **CT10nnlo** PDF set. PDF choice validated on the observed weaker suppression of the strange quark in the W,Z cross-section data as published in [arXiv:1612.03016](https://arxiv.org/abs/1612.03016)

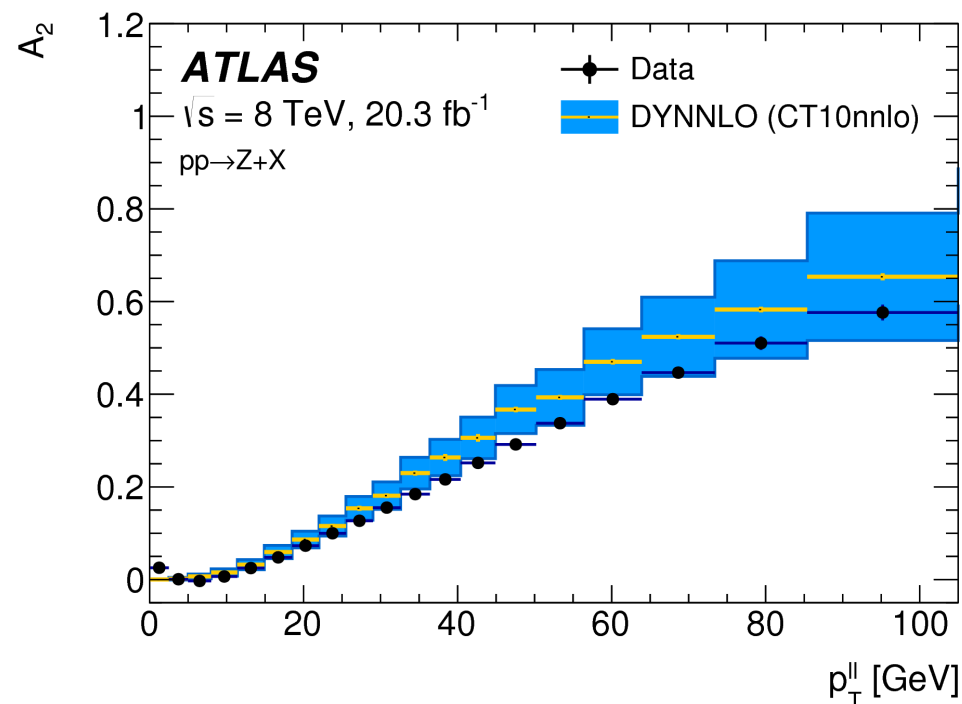
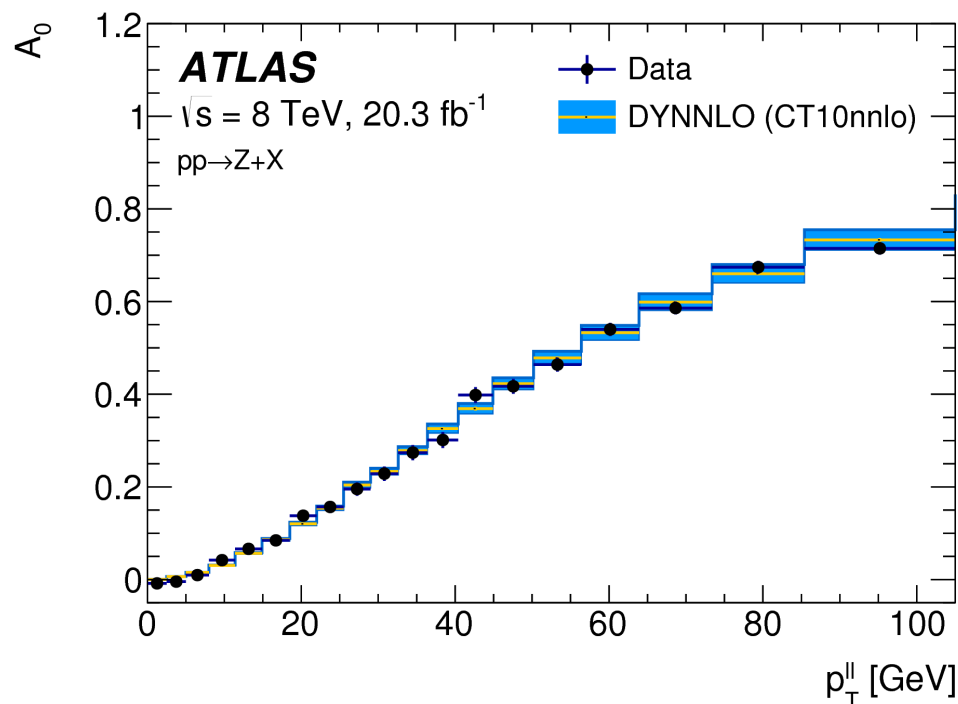


Satisfactory agreement between the theoretical prediction and the measurements is observed: $\chi^2/\text{dof} = 45/34$.

Polarisation coefficients

The A_i coefficients are modelled with fixed order pQCD at NNLO.

The predictions (DYNNLO) are validated by comparison to the A_i measurements in 8 TeV Z-boson data [JHEP08\(2016\)159](#)



Uncertainties on A_i modelling: experimental uncertainty of the measurement and observed discrepancy for A_2 coefficient

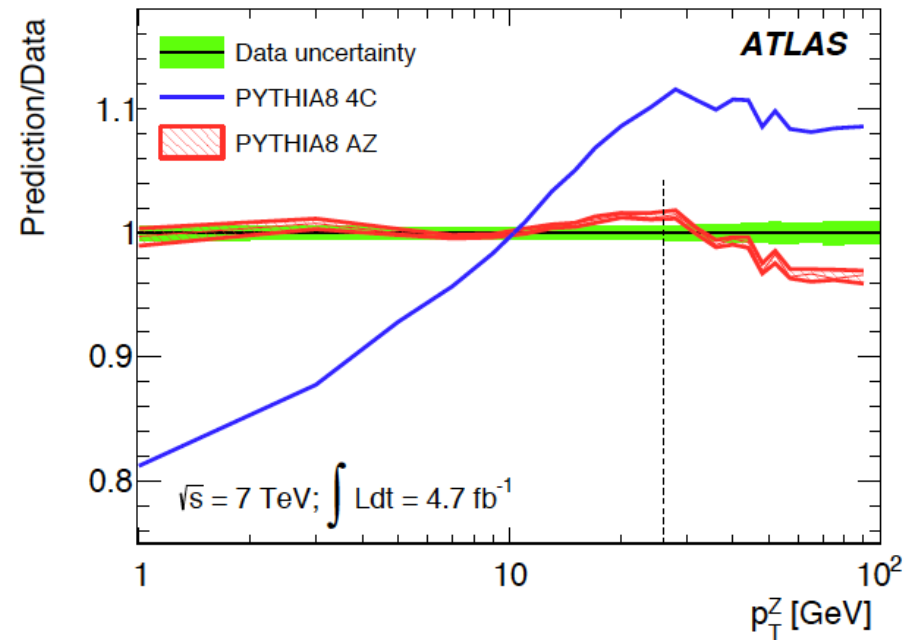
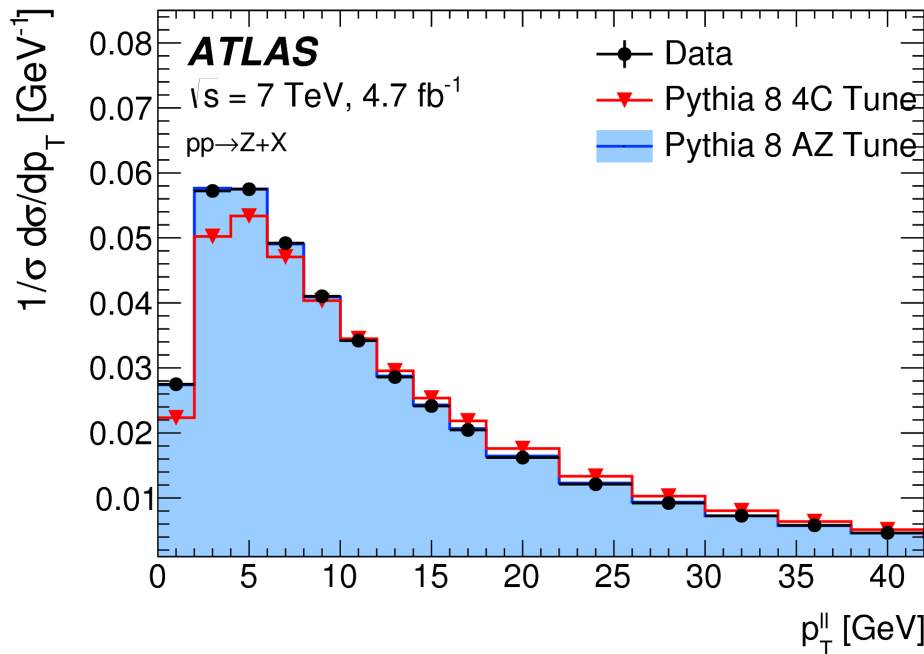
W -boson charge	W^+		W^-		Combined	
	p_T^ℓ	m_T	p_T^ℓ	m_T	p_T^ℓ	m_T
Angular coefficients	5.8	5.3	5.8	5.3	5.8	5.3

Z transverse momentum

Parton shower MC Pythia 8 tuned to the 7 TeV data AZ tune (better description in rapidity bins than the AZNLO tune of Powheg+Pythia) [JHEP09\(2014\)145](#)

The agreement between data and Pythia AZ is better than 1% for $p_T < 40$ GeV

PYTHIA8	
Tune Name	AZ
Primordial k_T [GeV]	1.71 ± 0.03
ISR $\alpha_S^{\text{ISR}}(m_Z)$	0.1237 ± 0.0002
ISR cut-off [GeV]	0.59 ± 0.08
$\chi^2_{\text{min}}/\text{dof}$	45.4/32



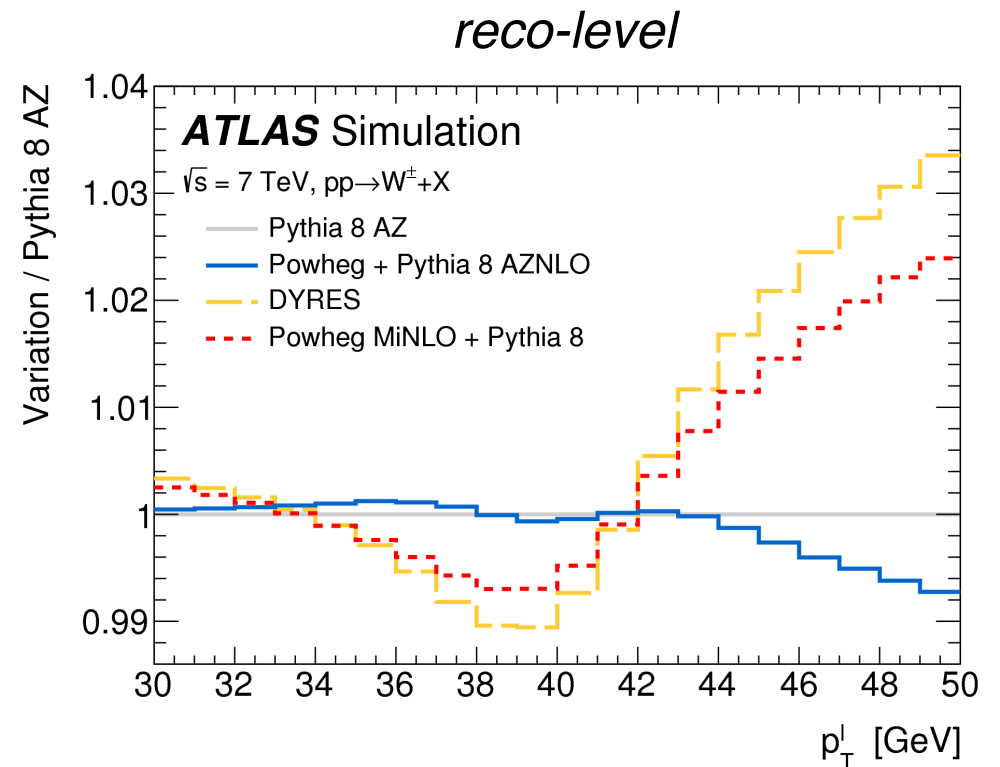
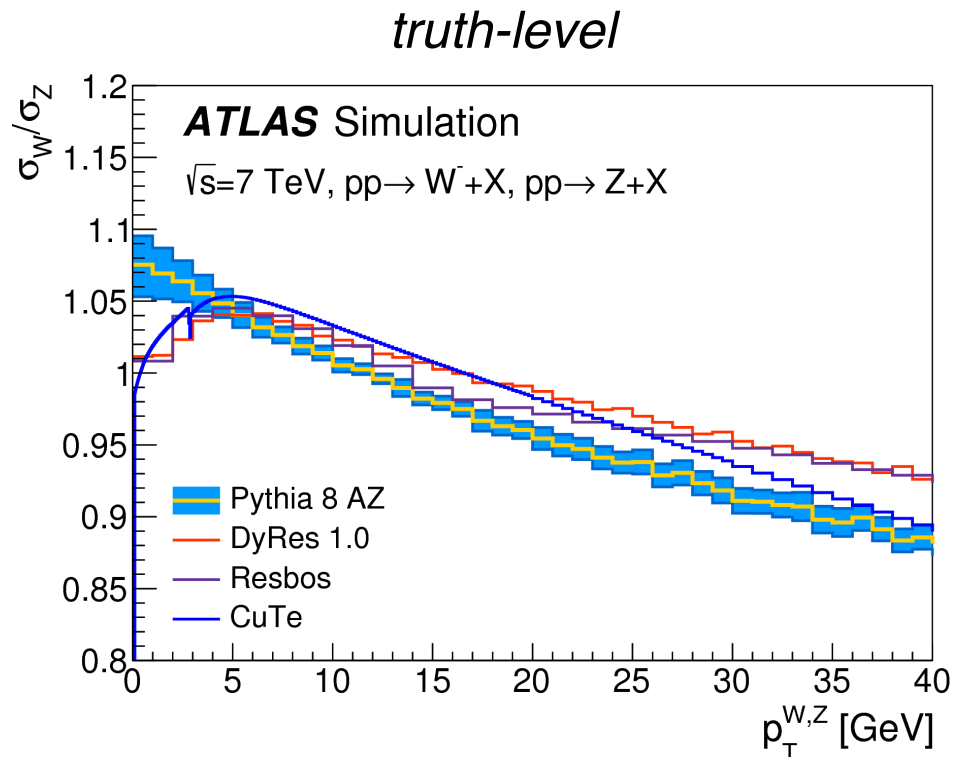
The accuracy of Z data is propagated and considered as an uncertainty

W-boson charge Kinematic distribution	W^+		W^-		Combined	
	p_T^ℓ	m_T	p_T^ℓ	m_T	p_T^ℓ	m_T
AZ tune	3.0	$_{28}^{3.4}$	3.0	3.4	3.0	3.4

W transverse momentum (I)

The Pythia8 AZ tune is fixed by the p_T^Z data; extrapolate to W considering relative variations of the W and Z p_T distributions.

Resummed predictions (DYRES, ResBos, CuTe) and Powheg MiNLO+Pythia8 were tried but they predict **harder W p_T spectrum for a given p_T (Z) spectrum.**

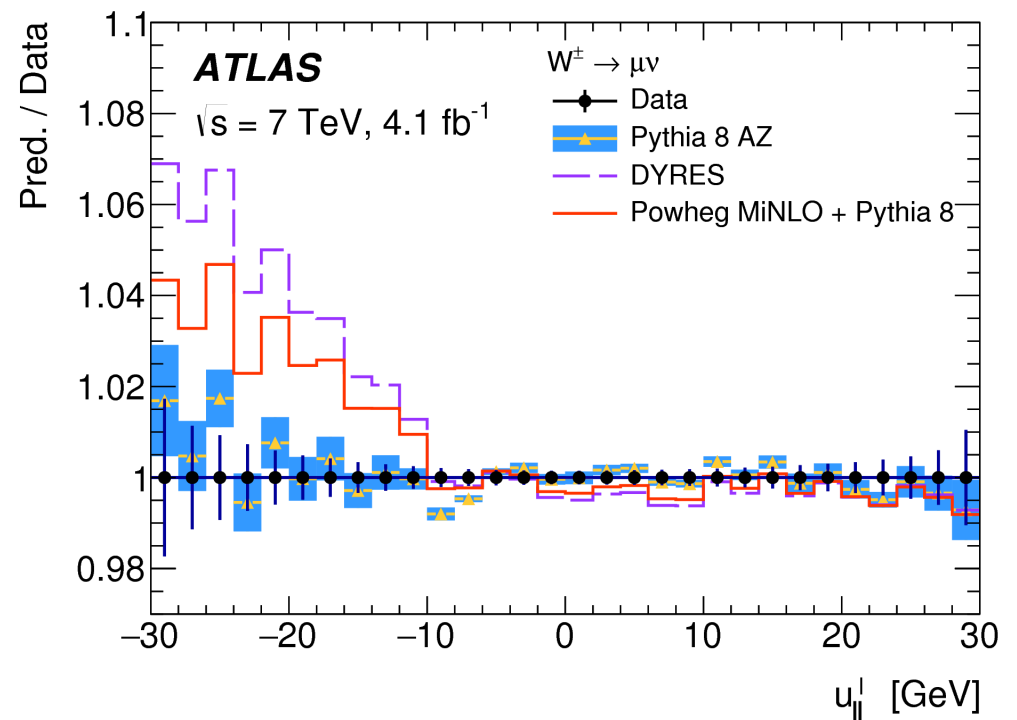
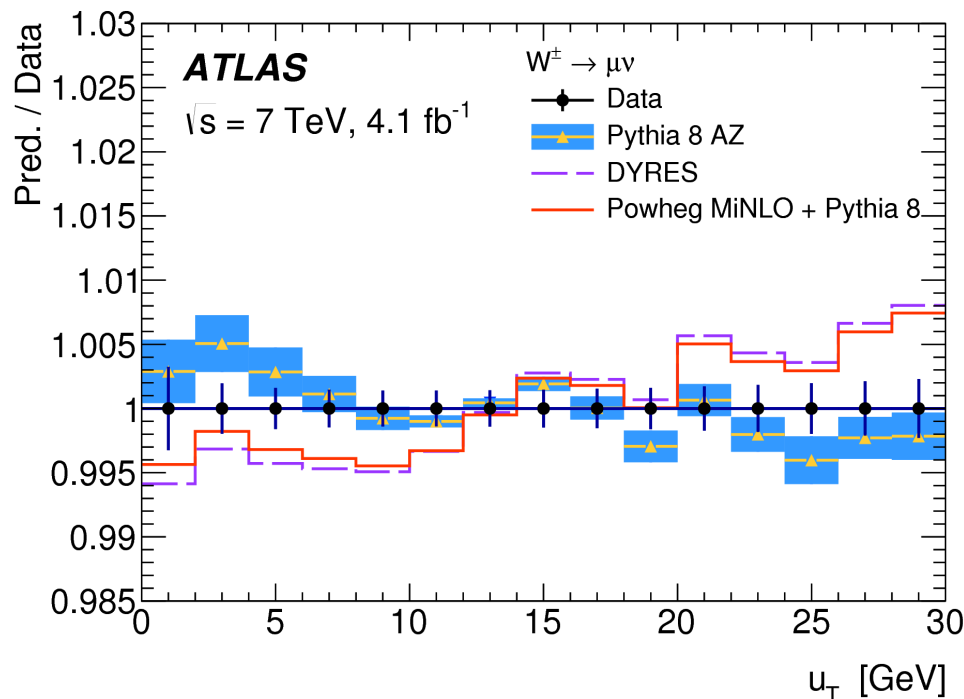


The effect on m_W of using the “formally” more accurate predictions has a significant impact on the W-mass value of the order of 50-100 MeV

W transverse momentum (II)

To validate the choice of Pythia8 AZ for the baseline, use u_{\parallel}^l distribution which is very sensitive to the underlying p_{T}^W distribution

—> provide a data-driven validation of the accuracy of our Pythia8 AZ model and compare to other calculations



NNLL resummed predictions and Powheg+MiNLO strongly disfavoured by the data however PS MC are in a good agreement; tested using Pythia8 , Herwig7 and Powheg+Pythia8

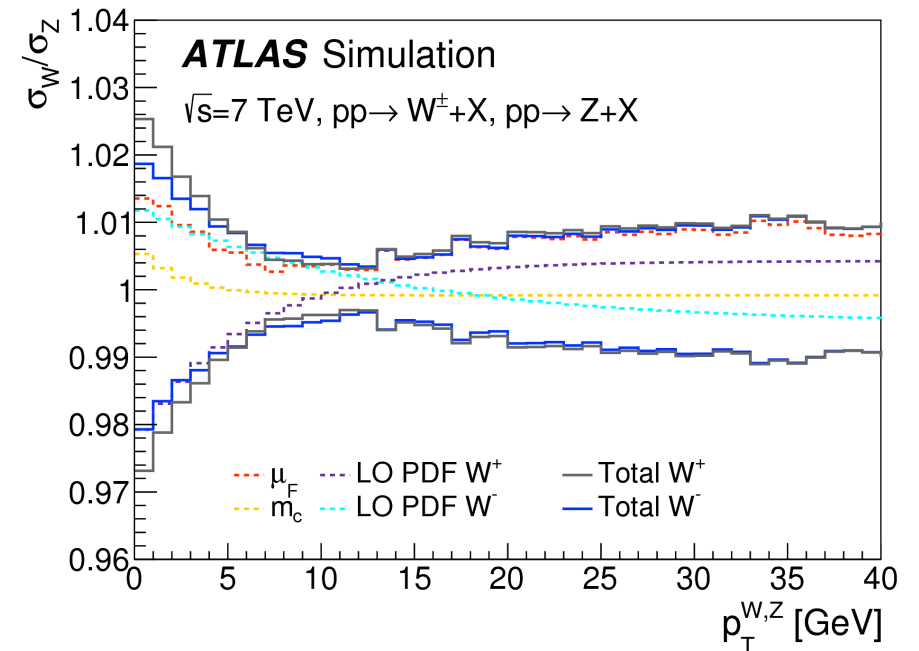
p_T^W uncertainties

Heavy flavour initiated production (HFI) introduces differences between Z and W and determines a harder p_T spectrum, expect certain degree of decorrelation. However higher-order QCD expected to be largely correlated between W and Z produced by **light quarks**

Consider relative variations on $p_T(W)/p_T(Z)$ under uncertainty variations.

Uncertainty: heavy quark mass variations (varying m_c by ± 0.5 GeV), factorisation scale variations in the QCD ISR (separately for light and heavy-quark induced production)

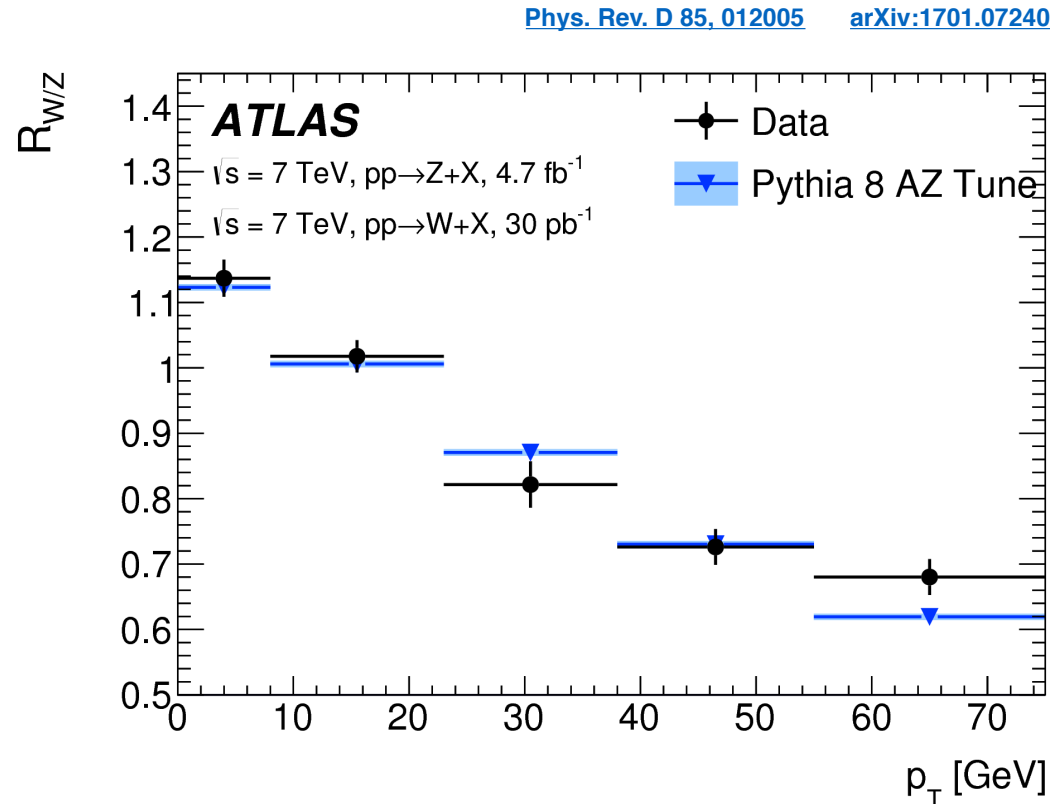
Largest deviation of $p_T(W)/p_T(Z)$ for the **parton shower PDF** variation: CTEQ6L1 LO (nominal) to CT14lo, MMHT2014lo and NNPDF2.3lo



W-boson charge Kinematic distribution	W^+		W^-		Combined	
	p_T^ℓ	m_T	p_T^ℓ	m_T	p_T^ℓ	m_T
Charm-quark mass	1.2	1.5	1.2	1.5	1.2	1.5
Parton shower μ_F with heavy-flavour decorrelation	5.0	6.9	5.0	6.9	5.0	6.9
Parton shower PDF uncertainty	3.6	4.0	2.6	2.4	1.0	1.6

Reducing p_T^W uncertainties

The ratio of the W and Z p_T distributions has been measured



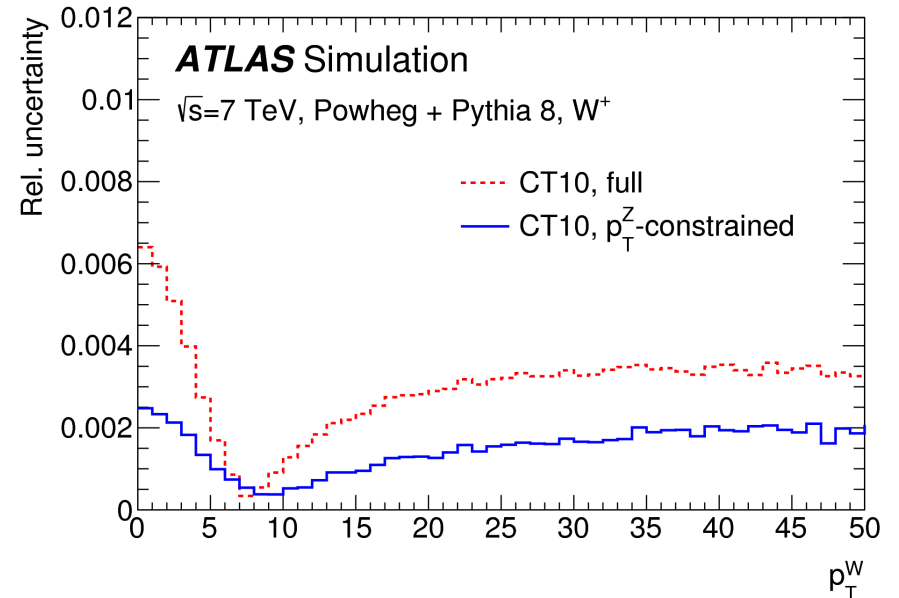
Limited precision of the data ($\sim 3\%$), and broad bin width ($\sim 8 \text{ GeV}$) limit the impact of these measurements on the systematic uncertainty.

Further measurements would be useful, ideally with low pile-up, targeting bin width $< 5 \text{ GeV}$ and a precision about $\sim 1\%$.

PDF uncertainties

PDF variations (25 error eigenvectors) of CT10nnlo are applied simultaneously to the boson rapidity, A_i , and p_T distributions.

Only relative variations of the $p_T(W)$ and $p_T(Z)$ induced by PDFs are considered.



W-boson charge Kinematic distribution	W^+		W^-		Combined	
	p_T^ℓ	m_T	p_T^ℓ	m_T	p_T^ℓ	m_T
Fixed-order PDF uncertainty	13.1	14.9	12.0	14.2	8.0	8.7

The PDF uncertainties are very similar between p_T^ℓ and m_T but strongly *anti-correlated between W^+ and W^-* . Envelope taken from *CT14 and MMHT2014* ~ 3.8 MeV.

Summary of physics modelling uncertainties

	W^+		W^-		Combined	
	p_T^ℓ	m_T	p_T^ℓ	m_T	p_T^ℓ	m_T
W -boson charge						
Kinematic distribution						
δm_W [MeV]						
Fixed-order PDF uncertainty	13.1	14.9	12.0	14.2	8.0	8.7
AZ tune	3.0	3.4	3.0	3.4	3.0	3.4
Charm-quark mass	1.2	1.5	1.2	1.5	1.2	1.5
Parton shower μ_F with heavy-flavour decorrelation	5.0	6.9	5.0	6.9	5.0	6.9
Parton shower PDF uncertainty	3.6	4.0	2.6	2.4	1.0	1.6
Angular coefficients	5.8	5.3	5.8	5.3	5.8	5.3
Total	15.9	18.1	14.8	17.2	11.6	12.9

QCD

Decay channel	$W \rightarrow e\nu$		$W \rightarrow \mu\nu$	
	p_T^ℓ	m_T	p_T^ℓ	m_T
δm_W [MeV]				
FSR (real)	< 0.1	< 0.1	< 0.1	< 0.1
Pure weak and IFI corrections	3.3	2.5	3.5	2.5
FSR (pair production)	3.6	0.8	4.4	0.8
Total	4.9	2.6	5.6	2.6

EW

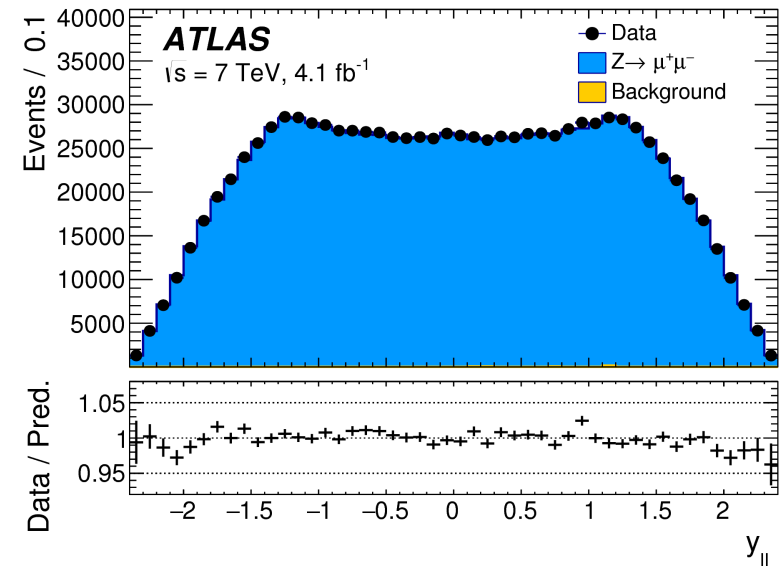
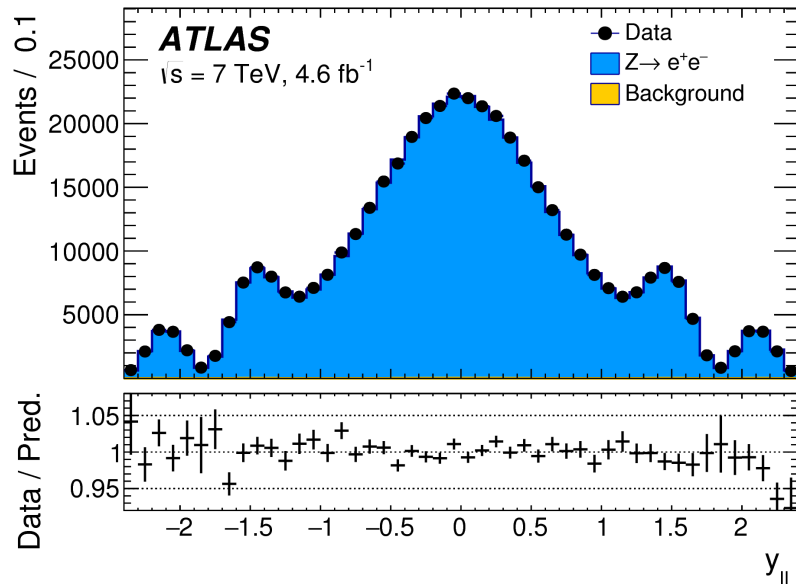
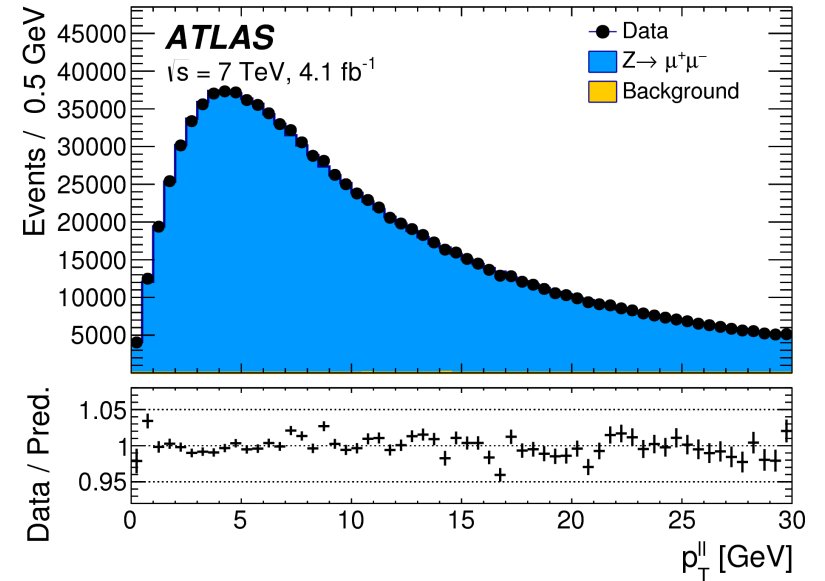
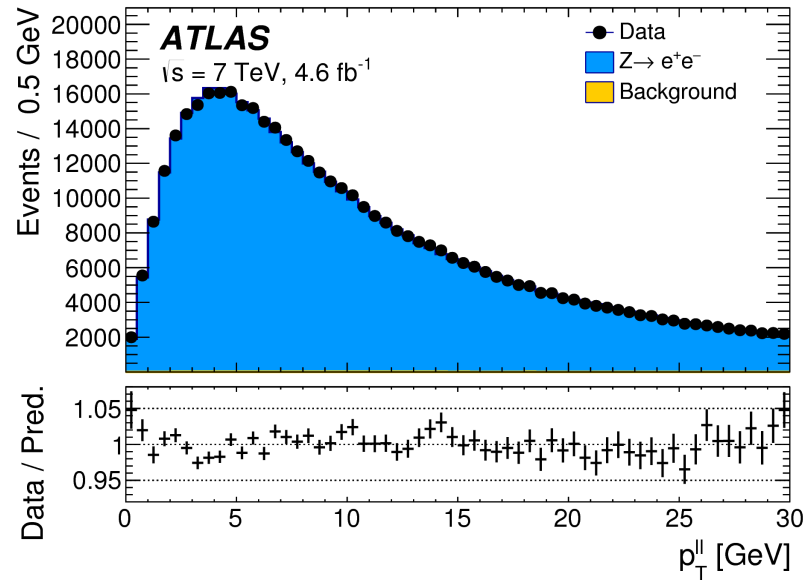
The PDF uncertainties are the dominant followed by $p_T(W)$ uncertainty due to the heavy-flavour initiated production.

Validation and results



Z control distributions: p_T , y

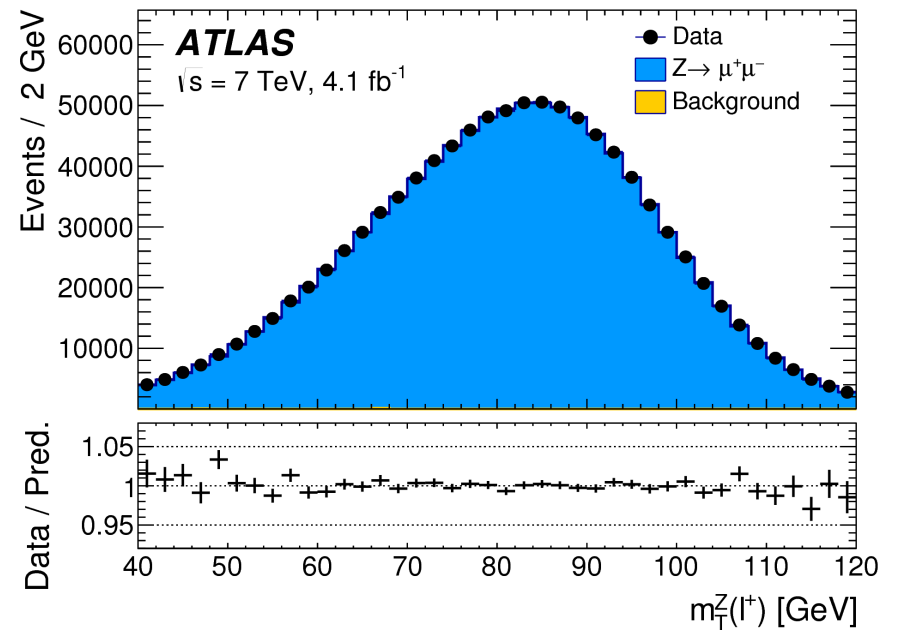
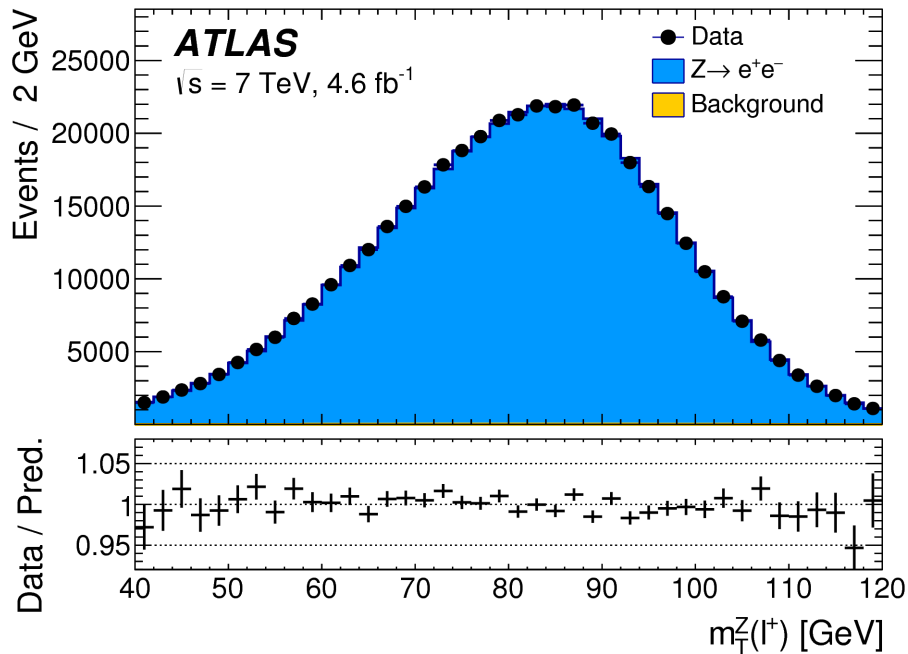
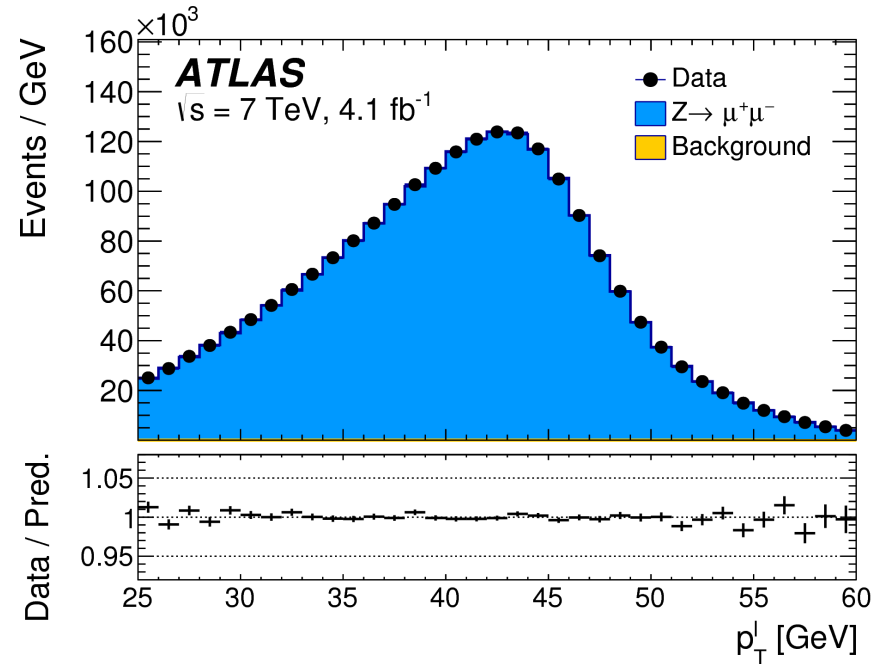
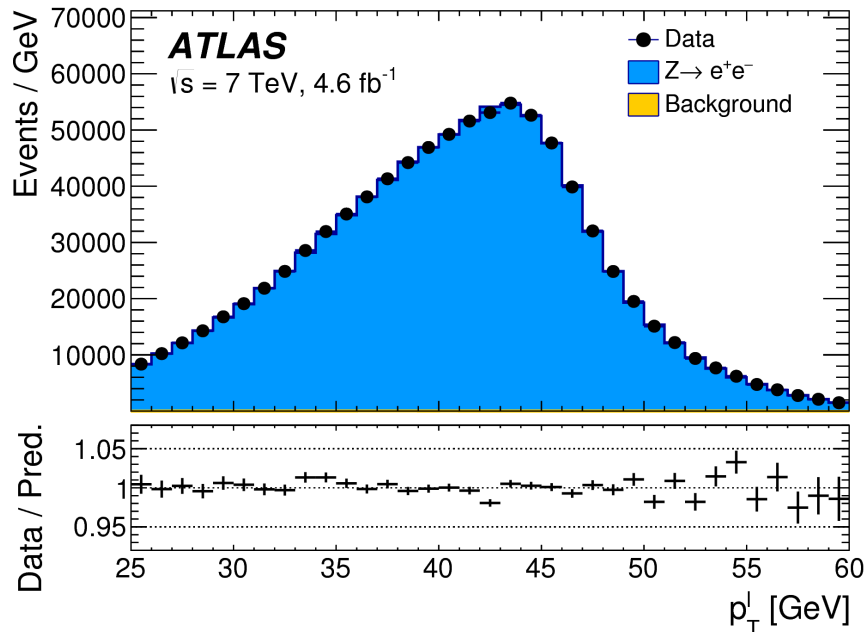
Z transverse momentum and rapidity distributions in e , μ channels



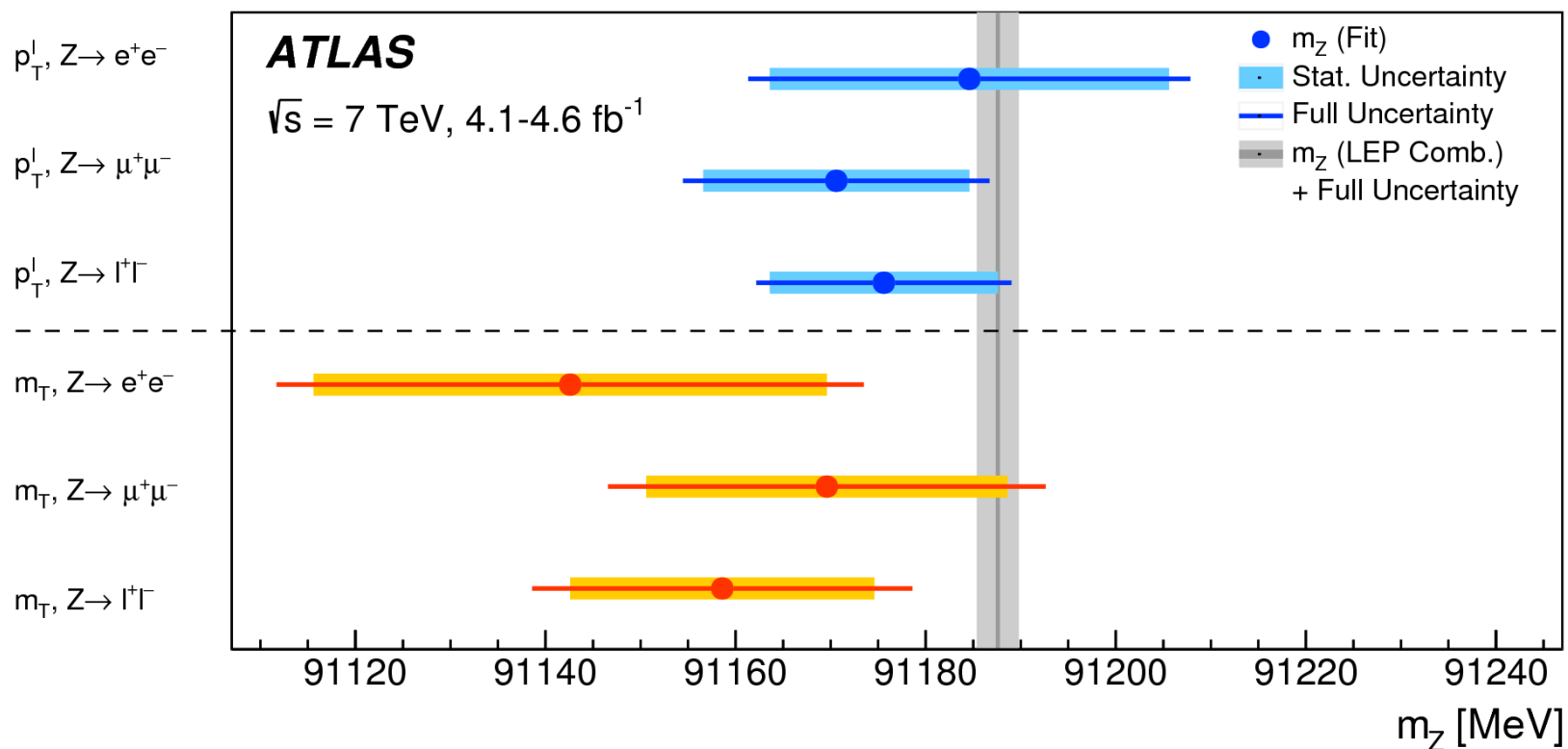
Good agreement is observed. Error bars are statistics only.

Z mass-sensitive distributions: p_T^l and m_{T^l}

Transverse momentum and transverse mass distributions in e, μ channels



Z mass



Lepton charge Distribution	ℓ^+		ℓ^-		Combined	
	p_T^ℓ	m_T	p_T^ℓ	m_T	p_T^ℓ	m_T
Δm_Z [MeV]			38			
$Z \rightarrow ee$	$13 \pm 31 \pm 10$	$-93 \pm 38 \pm 15$	$-20 \pm 31 \pm 10$	$4 \pm 38 \pm 15$	$-3 \pm 21 \pm 10$	$-45 \pm 27 \pm 15$
$Z \rightarrow \mu\mu$	$1 \pm 22 \pm 8$	$-35 \pm 28 \pm 13$	$-36 \pm 22 \pm 8$	$-1 \pm 27 \pm 13$	$-17 \pm 14 \pm 8$	$-18 \pm 19 \pm 13$
Combined	$5 \pm 18 \pm 6$	$-58 \pm 23 \pm 12$	$-31 \pm 18 \pm 6$	$1 \pm 22 \pm 12$	$-12 \pm 12 \pm 6$	$-29 \pm 16 \pm 12$

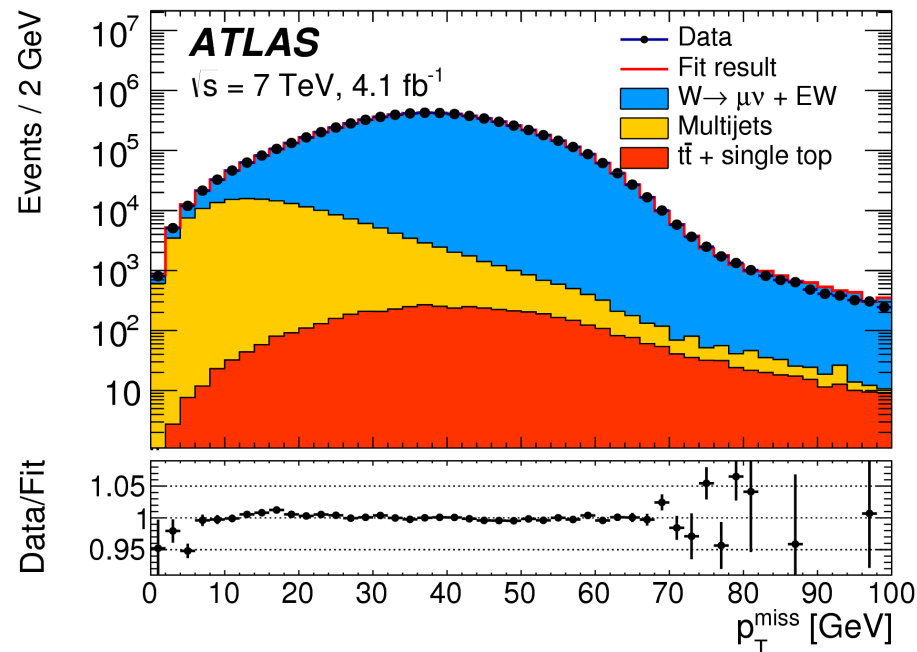
Results are consistent with the combined LEP value of m_Z within experimental uncertainties

Backgrounds in W

Electroweak and top-quark backgrounds are determined from simulation

Multijet background is determined using data-driven techniques:

- define background-dominated fit regions with relaxed cuts of the event selection
- template fits in these regions to 3 observables: p_T^{miss} , m_T and p_T^ℓ/m_T
- control regions are obtained by inverting the lepton isolation requirements



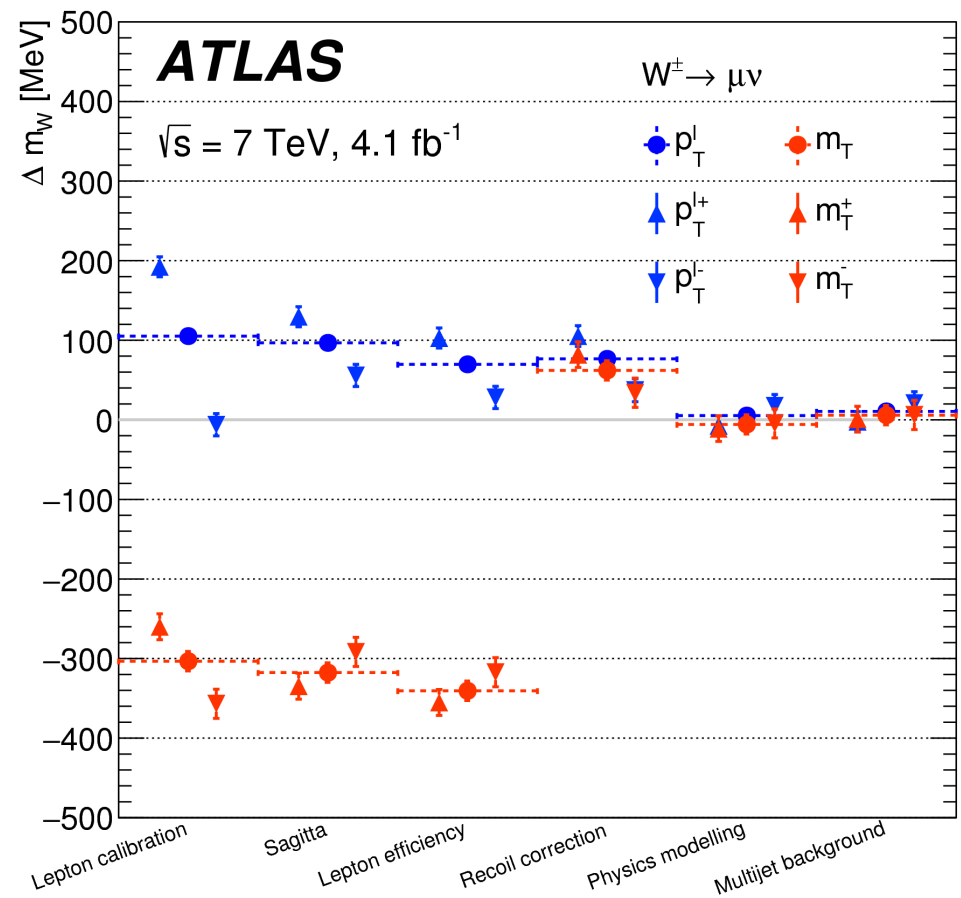
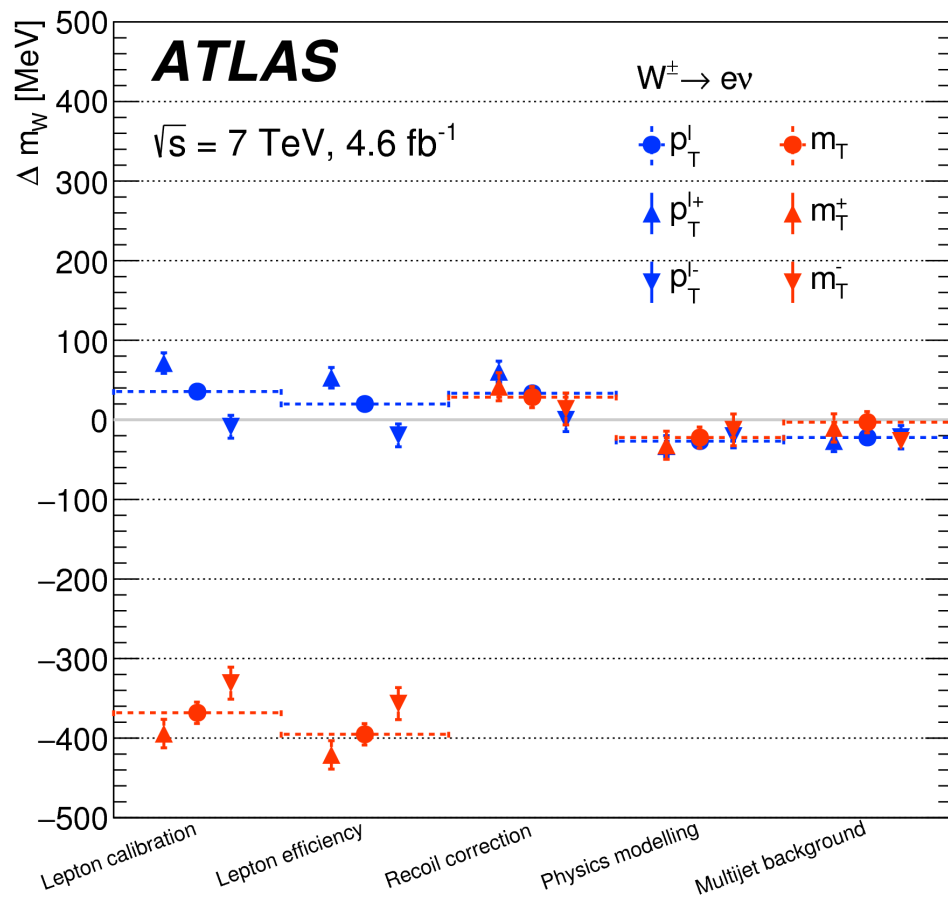
$W \rightarrow \mu\nu$						
Category	$W \rightarrow \tau\nu$	$Z \rightarrow \mu\mu$	$Z \rightarrow \tau\tau$	Top	Dibosons	Multijet
W^\pm $0.0 < \eta < 0.8$	1.04	2.83	0.12	0.16	0.08	0.72
W^\pm $0.8 < \eta < 1.4$	1.01	4.44	0.11	0.12	0.07	0.57
W^\pm $1.4 < \eta < 2.0$	0.99	6.78	0.11	0.07	0.06	0.51
W^\pm $2.0 < \eta < 2.4$	1.00	8.50	0.10	0.04	0.05	0.50
W^\pm all η bins	1.01	5.41	0.11	0.10	0.06	0.58
W^+ all η bins	0.99	4.80	0.10	0.09	0.06	0.51
W^- all η bins	1.04	6.28	0.14	0.12	0.08	0.68

$W \rightarrow e\nu$						
Category	$W \rightarrow \tau\nu$	$Z \rightarrow ee$	$Z \rightarrow \tau\tau$	Top	Dibosons	Multijet
W^\pm $0.0 < \eta < 0.6$	1.02	3.34	0.13	0.15	0.08	0.59
W^\pm $0.6 < \eta < 1.2$	1.00	3.48	0.12	0.13	0.08	0.76
W^\pm $1.8 < \eta < 2.4$	0.97	3.23	0.11	0.05	0.05	1.74
W^\pm all η bins	1.00	3.37	0.12	0.12	0.07	1.00
W^+ all η bins	0.98	2.92	0.10	0.11	0.06	0.84
W^- all η bins	1.04	3.98	0.14	0.13	0.08	1.21

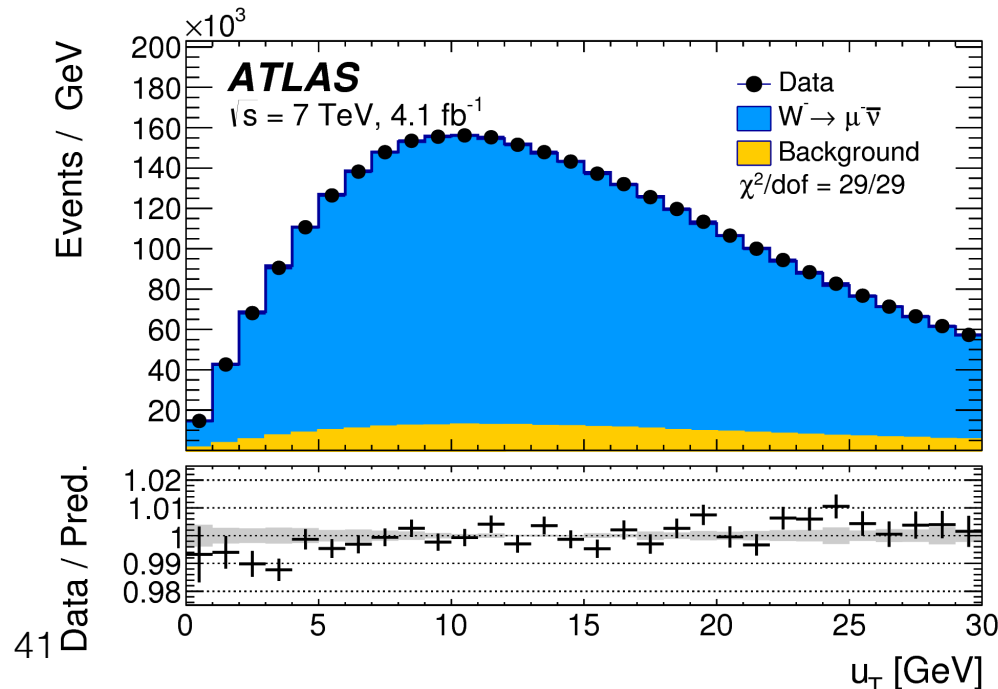
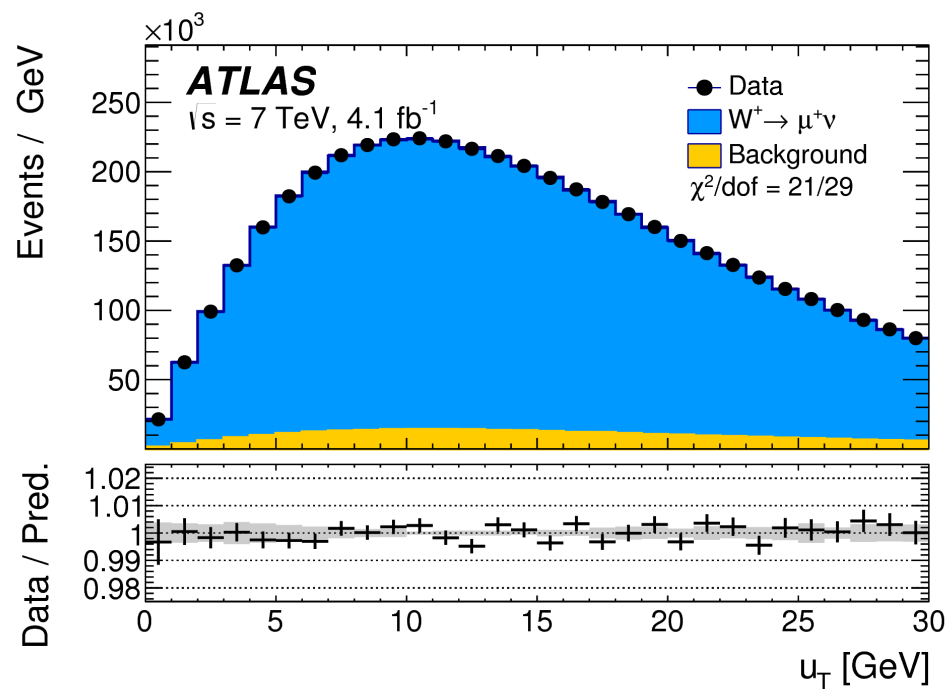
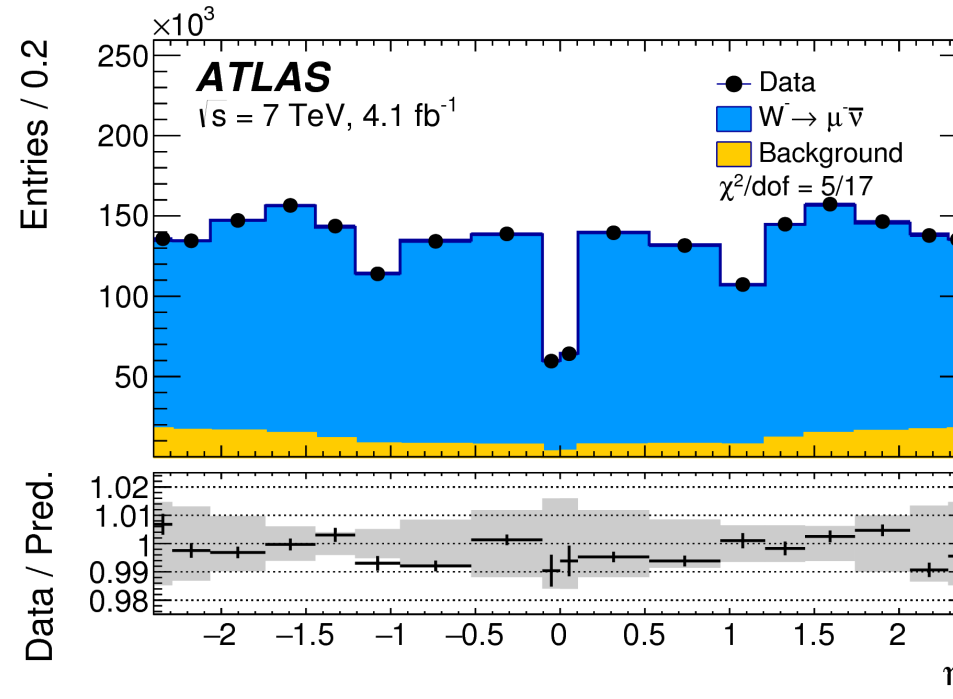
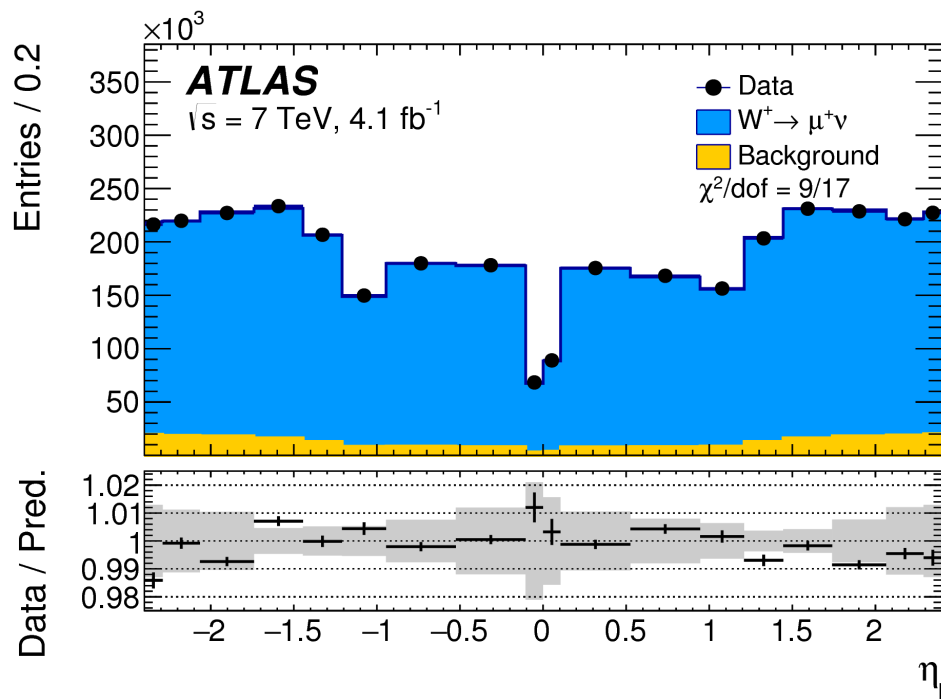
Kinematic distribution	p_T^ℓ				m_T			
	$W \rightarrow e\nu$		$W \rightarrow \mu\nu$		$W \rightarrow e\nu$		$W \rightarrow \mu\nu$	
Decay channel	W^+	W^-	W^+	W^-	W^+	W^-	W^+	W^-
W-boson charge	W^+	W^-	W^+	W^-	W^+	W^-	W^+	W^-
δm_W [MeV]								
$W \rightarrow \tau\nu$ (fraction, shape)	0.1	0.1	0.1	0.2	0.1	0.2	0.1	0.3
$Z \rightarrow ee$ (fraction, shape)	3.3	4.8	-	-	4.3	6.4	-	-
$Z \rightarrow \mu\mu$ (fraction, shape)	-	-	3.5	4.5	-	-	4.3	5.2
$Z \rightarrow \tau\tau$ (fraction, shape)	0.1	0.1	0.1	0.2	0.1	0.2	0.1	0.3
WW, WZ, ZZ (fraction)	0.1	0.1	0.1	0.1	0.4	0.4	0.3	0.4
Top (fraction)	0.1	0.1	0.1	0.1	0.3	0.3	0.3	0.3
Multijet (fraction)	3.2	3.6	1.8	2.4	8.1	8.6	3.7	4.6
Multijet (shape)	3.8	3.1	1.6	1.5	8.6	8.0	2.5	2.4
Total	6.0	6.8	4.3	5.3	12.6	13.4	6.2	7.4

Summary of corrections

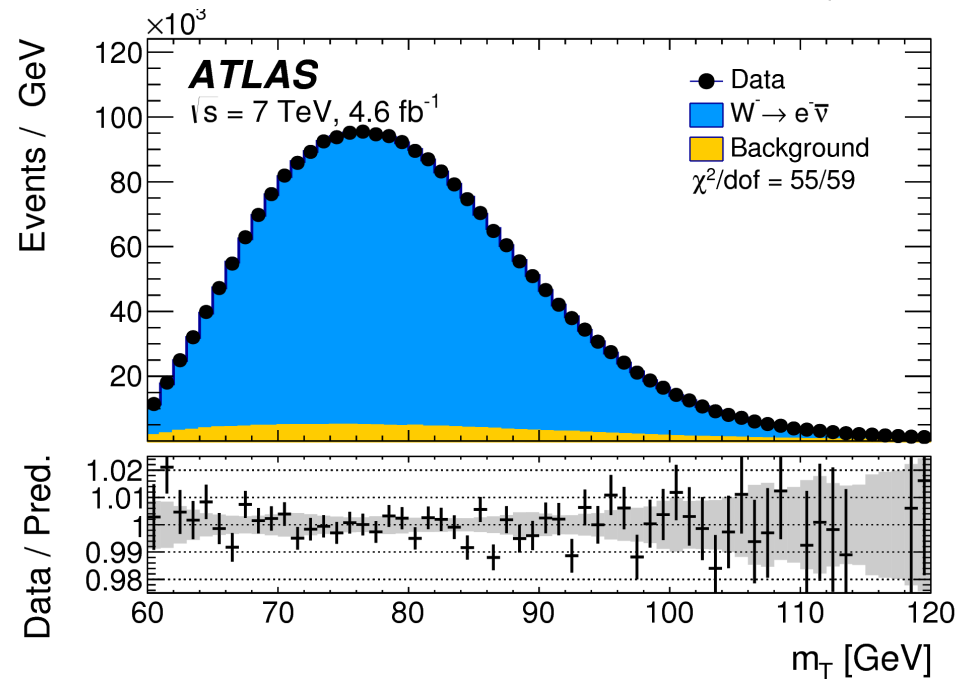
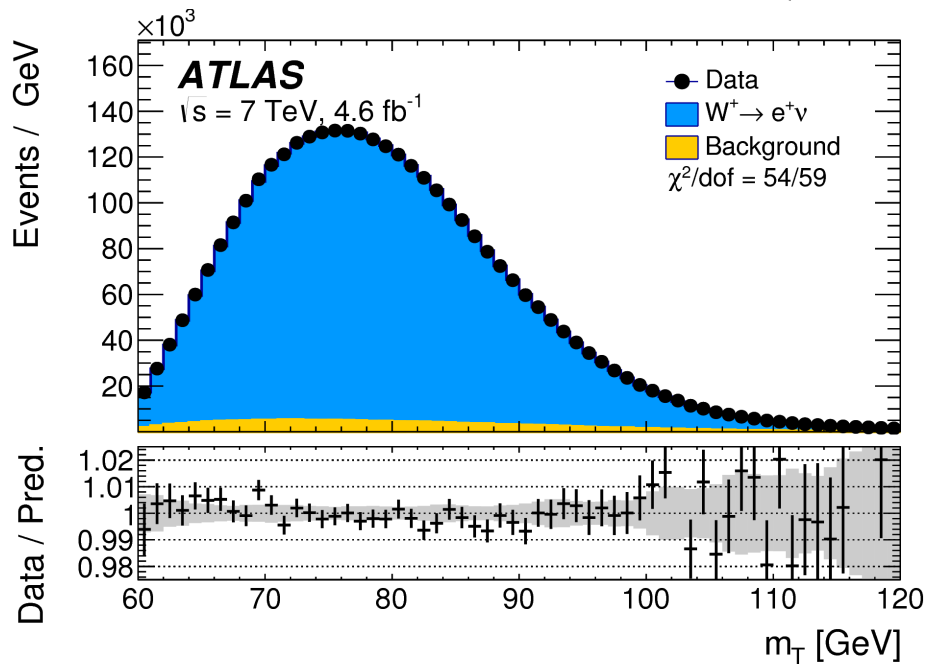
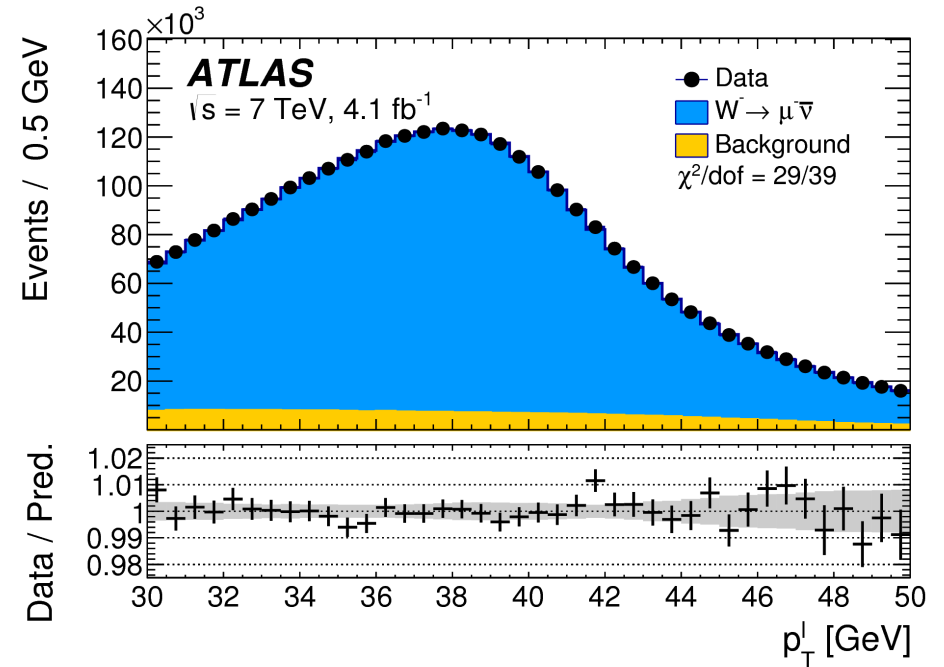
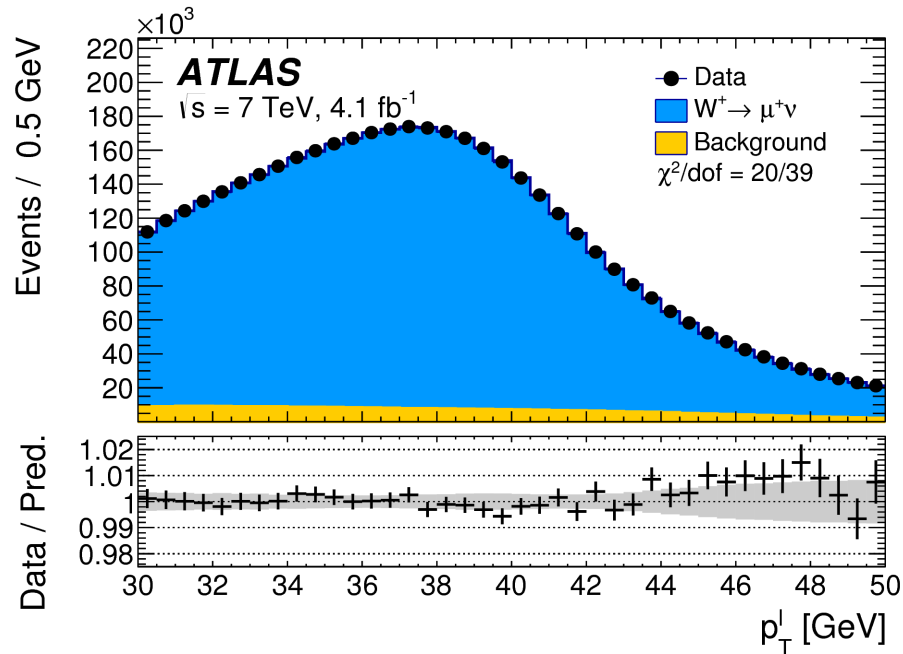
After all corrections are applied, **consistent results** are achieved between different channels, observables, categories, charges and only after, results were unblinded.



W control distributions: η , p_T

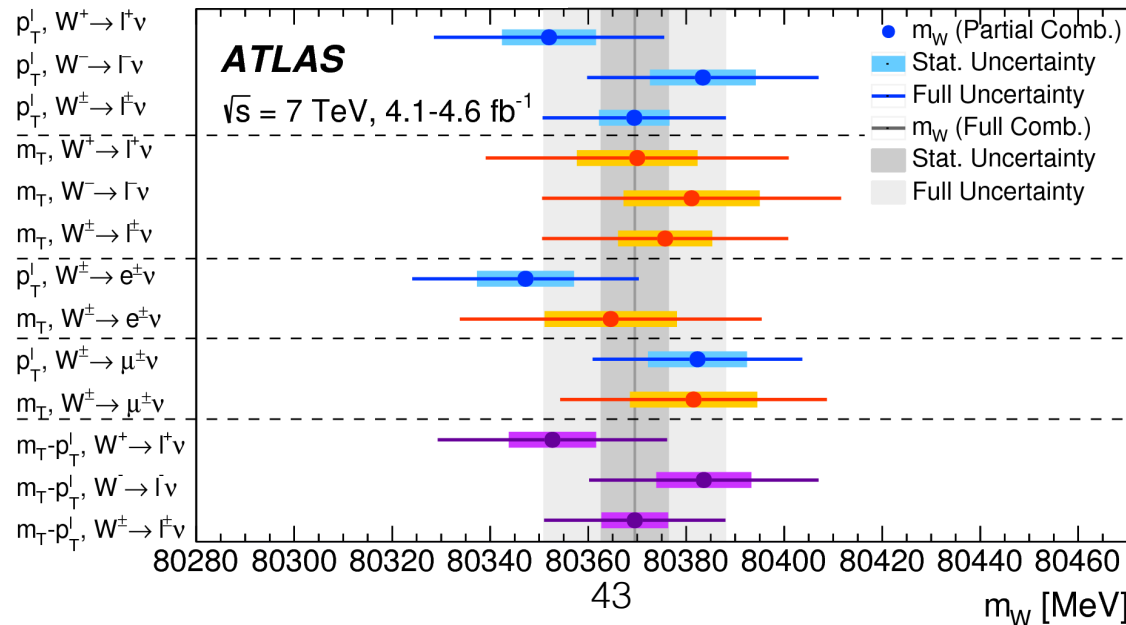
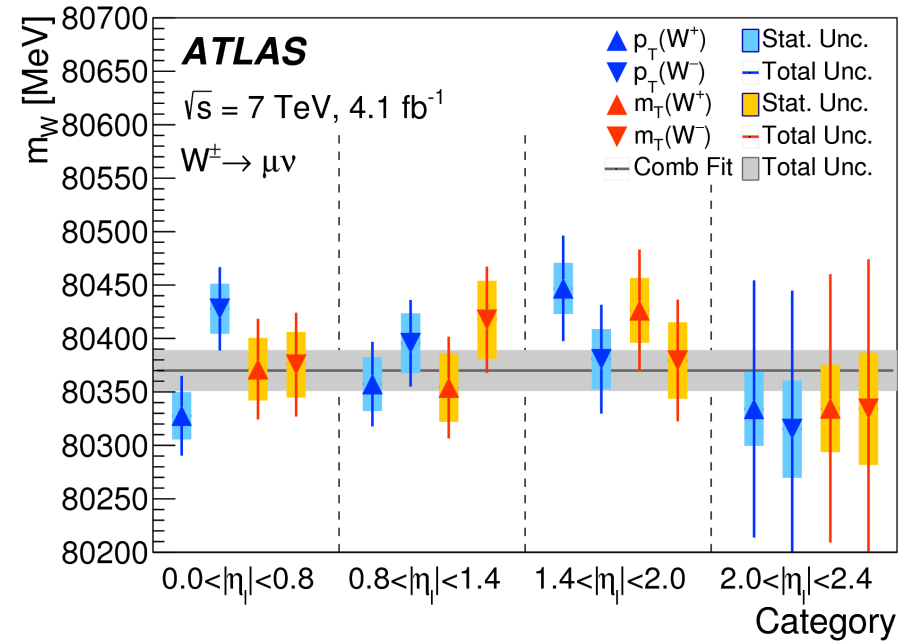
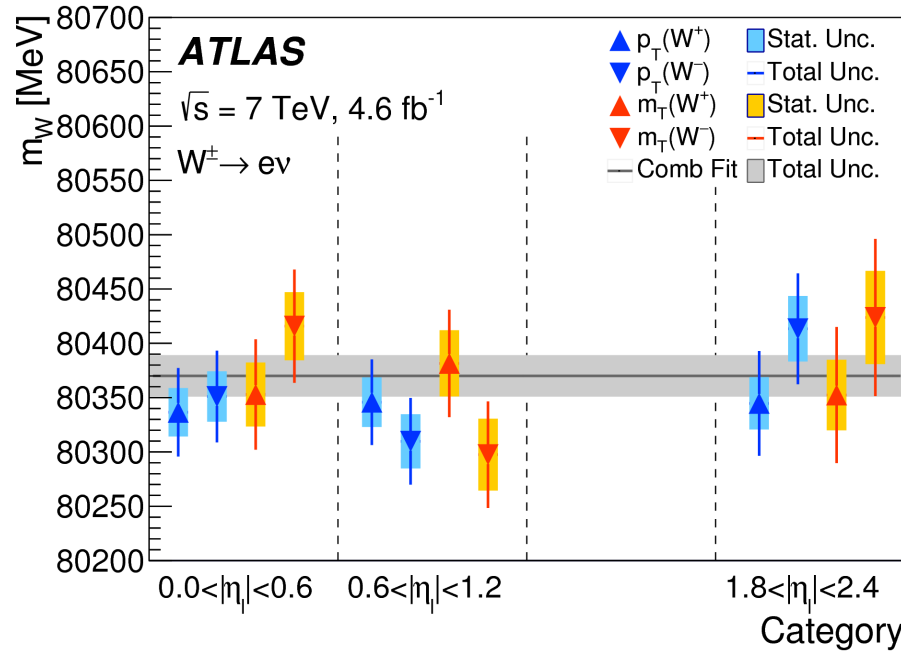


W mass-sensitive distributions: p_T^l and m_T



Consistency of the results

The consistency of the results was checked in the different categories but also in different pileup, u_T and $u_{||}$ bins



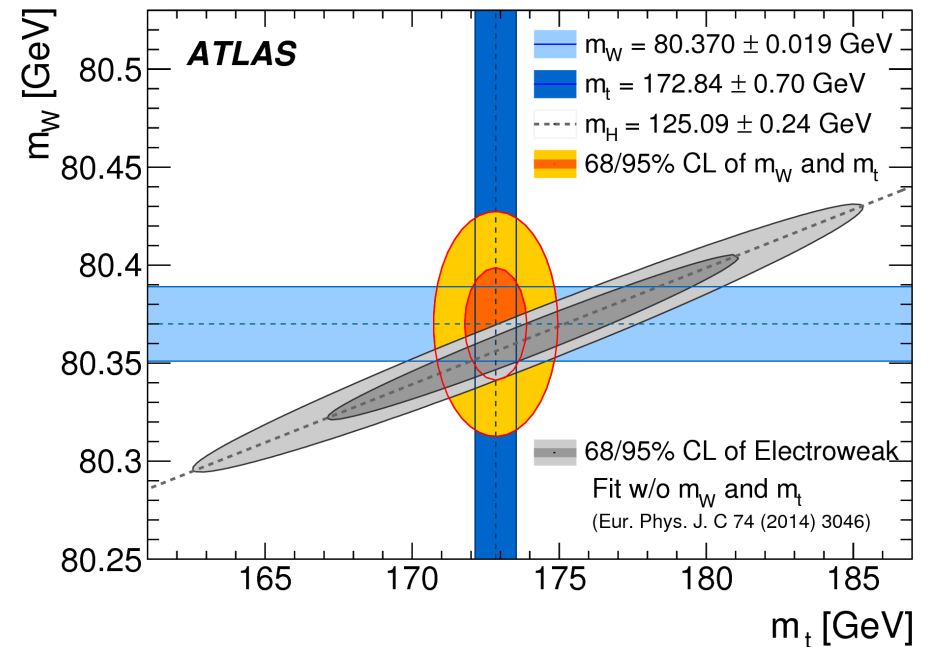
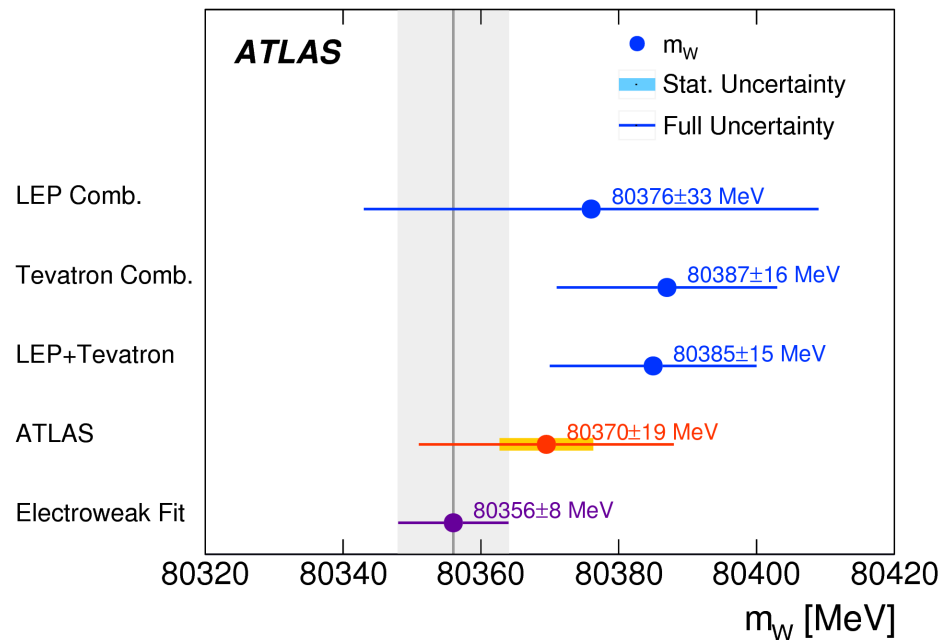
Fitting ranges:
 $32 < p_T^l < 45 \text{ GeV}$,
 $66 < m_T < 99 \text{ GeV}$

Results

$$m_W = 80369.5 \pm 6.8 \text{ MeV (stat.)} \pm 10.6 \text{ MeV (exp. syst.)} \pm 13.6 \text{ MeV (mod. syst.)}$$

$$= 80369.5 \pm 18.5 \text{ MeV,}$$

Combined categories	Value [MeV]	Stat. Unc.	Muon Unc.	Elec. Unc.	Recoil Unc.	Bckg. Unc.	QCD Unc.	EWK Unc.	PDF Unc.	Total Unc.	χ^2/dof of Comb.
$m_T-p_T^\ell, W^\pm, e-\mu$	80369.5	6.8	6.6	6.4	2.9	4.5	8.3	5.5	9.2	18.5	29/27

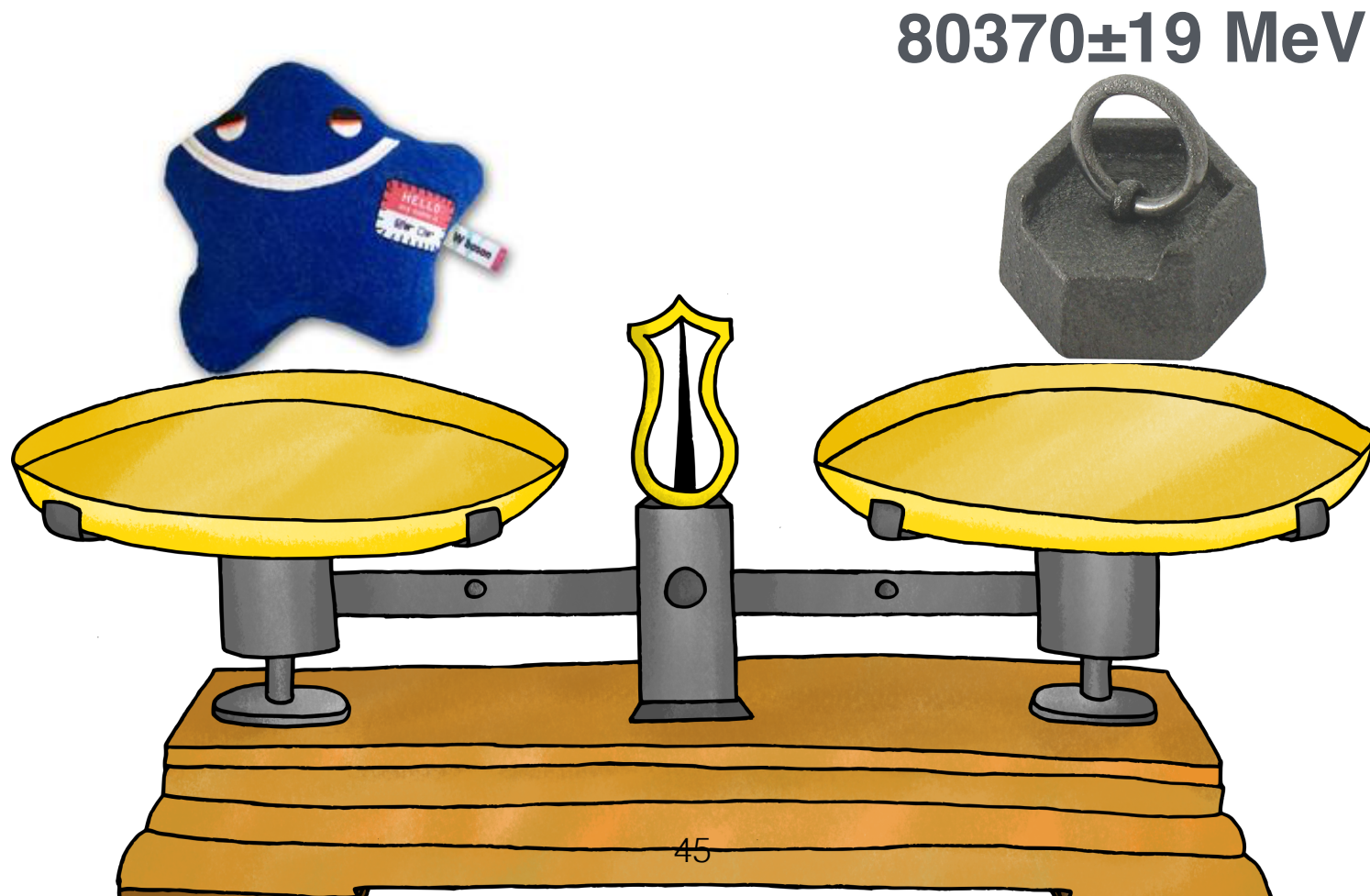


The result is consistent with the **SM expectation**, compatible with the world average and **competitive in precision** to the currently leading measurements by CDF and D0

Conclusion

The first LHC measurement of $m_W = 80370 \pm 19 \text{ MeV}$ is public now [arXiv:1701.07240v1](#) after many years of effort in the ATLAS collaboration.

The central value is consistent with the SM prediction and with the current world average value.



Perspectives

The uncertainty is dominated by theoretical modelling uncertainties, therefore more work in this direction is required and *a fully consistent model within one simulation tool* is needed.

The W mass measurement in CMS is ongoing. A first W -like measurement of the Z mass was performed.

More data are available with the **8 and 13 TeV** datasets which can be used to improve the analysis and to further constrain the PDFs.

Experimentally, with the increase of the statistics in Z sample, most of the calibration uncertainties can be reduced. While more work is needed on the recoil with the increasing pileup.